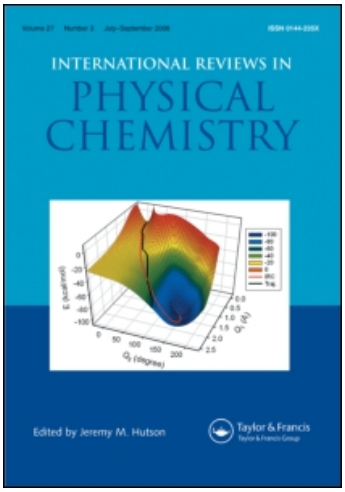


**International Reviews in Physical Chemistry**
Publication details, including instructions for authors and subscription information:
http://www.informaworld.com/smpp/title~content=t713724383

# Laser Stark spectroscopy

Geoffrey Duxbury[a]
[a] Department of Physics, University of Strathclyde, Glasgow, Scotland

**To cite this Article** Duxbury, Geoffrey(1985) 'Laser Stark spectroscopy', International Reviews in Physical Chemistry, 4: 3, 237 — 278
**To link to this Article: DOI:** 10.1080/01442358509353361
**URL:** http://dx.doi.org/10.1080/01442358509353361

INTERNATIONAL REVIEWS IN PHYSICAL CHEMISTRY, 1985, VOL. 4, NO. 3, 237–278

# Laser Stark spectroscopy

By GEOFFREY DUXBURY
Department of Physics, University of Strathclyde,
107 Rottenrow, Glasgow G4 0NG, Scotland

This paper discusses the development of laser Stark spectroscopy (or laser electric resonance spectroscopy) in which transitions between molecular energy levels are tuned into resonance with fixed frequency molecular gas lasers. Emphasis is laid on the fundamentals of the method, and its extensions to sub-Doppler resolution, including optical–optical double resonance and level crossing. Examples of the use of these methods are chosen from three main areas; the study of the vibrational dependence of molecular dipole moments, the elucidation of the effects of collisional energy transfer, and the detection of the spectra of semi-stable molecules.



## 1. Introduction

The effect of an electric field on the optical spectra of an atom was first described by Johannes Stark (1913). Since then, the Stark effect has been an important tool in the investigation of atomic and molecular spectra. A comprehensive picture of this period from the earliest developments up to the start of laser spectroscopy is provided in a review by Buckingham (1972). In the present review we will be concerned only with laser spectroscopy, and in particular with laser electric resonance or laser Stark spectroscopy.

Laser Stark spectroscopy utilizes the Stark effect to shift transitions between molecular vibration–rotation energy levels into resonance with lasers whose frequencies are close to the zero-field transition frequency. This allows high-resolution spectroscopy to be accomplished with fixed frequency or slightly tunable lasers. It is one of the two main methods introduced in the period from 1965 to 1970, the other being laser magnetic resonance (L.M.R.) which uses the Zeeman effect for tuning. These methods were introduced because at that time no widely tunable lasters were available in the infrared and far infrared regions of the spectrum. Fujio Shimizu, one of the pioneers in this area, clearly regarded laser Stark spectroscopy as a stopgap until tunable lasers became available (Shimizu 1970 a). The resonance methods have survived the introduction of tunable lasers for three main reasons: their sensitivity for detecting low concentrations of reactive species, the resolution provided by using the high power of the lasers for saturation spectroscopy, and the ease of calibration of the systems. This last point is an important one since the shifts are measured relative to the positions of the laser lines whose frequencies have been accurately determined (Freed *et al.* 1980, Dale *et al.* 1979, Whitford *et al.* 1975), and hence some of the calibration problems found with the use of tunable lasers are automatically avoided.

The origins of laser Stark spectroscopy lie in some experiments carried out in Shimoda's group in Japan in 1967 (Sakurai *et al.* 1967). They showed that it was possible to generate uniform electrostatic fields of up to 50 kV $cm^{-1}$ in cells containing electrodes with narrow spacings ranging from 0·5 to 4 mm. Fields produced in this way

are sufficient to cause splittings of several GHz in the absorption lines of gases such as formaldehyde, in which nearly first-order Stark effects can be produced (Uehara *et al.* 1968), as shown in figure 1. Although the original experiments employed a He–Xe laser whose frequency was magnetically tuned, the first laser Stark experiments on $NH_3$ using fixed frequency submillimetre lasers and electrostatic tuning rapidly followed (Uehara *et al.* 1968, 1969) (figure 2). Fujio Shimuzu showed the power of the method by carrying out the systematic spectroscopy of the $v_2$ bands of $NH_3$ and $^{15}NH_3$ at Doppler-limited resolution, using fields up to $100\,kV\,cm^{-1}$ (1969, 1970a, b). At approximately the same time, Brewer and his colleagues (1969) demonstrated the use of the high power available from $CO_2$ lasers for saturation spectroscopy. They obtained Lamb dip spectra of $NH_2D$ in which the width of the saturation features was 1·5 MHz, figure 3, well inside the Doppler width of 80 MHz, and also carried out the first sub-Doppler optical–optical double resonance experiments using two $CO_2$ lasers. Experiments were also carried out by Duxbury and Jones in the submillimetre region (1971 a, b).



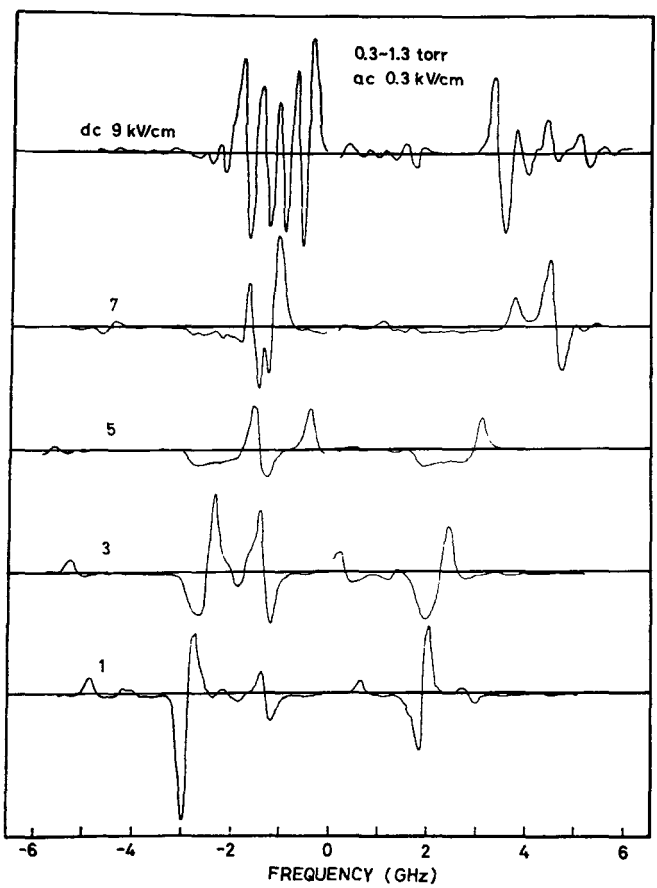


Figure 1. Stark modulation spectrum of HDCO around the $2850{\cdot}62\,cm^{-1}$ line of the HeXe laser. The laser frequency is tuned by the application of a magnetic field parallel to the axis of the laser tube. The Stark field is perpendicular to the optical field. (Reproduced by permission from *I.E.E.E. Journal of Quantum Electronics*, 1968, Q.E. **4**, 730.)

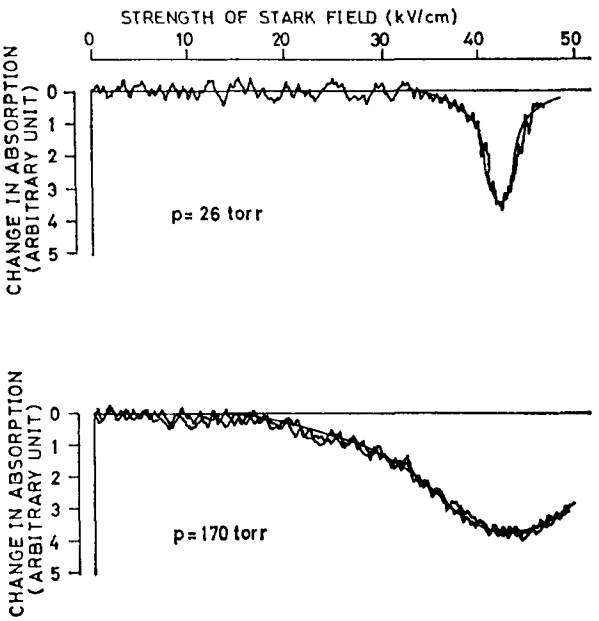


Figure 2. Observed and calculated Stark patterns of $NH_3$ using the 1747 GHz line of a pulsed electric discharge pumped $D_2O$ submillimetre laser. (Reproduced by permission from *I.E.E.E. Journal of Quantum Electronics*, 1968, Q.E. **4**, 731.)



Although in L.M.R. most of the early development was associated with the use of intracavity spectrometers based on submillimetre lasers (Evenson *et al.* 1980), in laser Stark spectroscopy most of the emphasis has been on experiments in the mid-infrared using $CO_2$ and CO lasers. One of the main reasons for this is associated with the methods used to produce the high fields needed for tuning. In L.M.R. the electromagnets used to produce the high magnetic fields of 1 to 2 T have a wide spacing of the pole pieces, typically 2 to 5 cm, and hence intracavity operation of submillimetre laser-band spectrometers is feasible. However, in laser Stark spectroscopy the high fields are usually produced by using flat steel or metallized glass plates held accurately parallel with a spacing of between 1 and 4 mm. This imposes severe limitations on the propagation of long wavelength laser radiation through the cells, and precludes intracavity operation in the submillimetre region.

Laser Stark spectroscopy relies on the identification of key patterns in the complex resonance spectra that are usually observed. This is most easily accomplished when the molecules being studied are either symmetric or nearly symmetric rotors, and when the vibration–rotation bands are isolated and hence free from perturbations. These criteria were met in the analyses of the electric resonance spectra of the $\nu_2$ band of formaldehyde (Johns and McKellar 1973) and the $\nu_3$ band of methyl fluoride (Herlemont *et al.* 1973, Freund *et al.* 1974) which were carried out in the period from 1972 to 1974. The work on methyl fluoride also illustrated the ready applicability of the Stark Lamb dip method to resolution enhancement (Freund *et al.* 1974).

Since these original experiments were carried out the method has been extended in several directions, for studying the spectra of semi-stable molecules, for measuring the spectra of non-polar molecules, and for measuring the vibrational and rotational

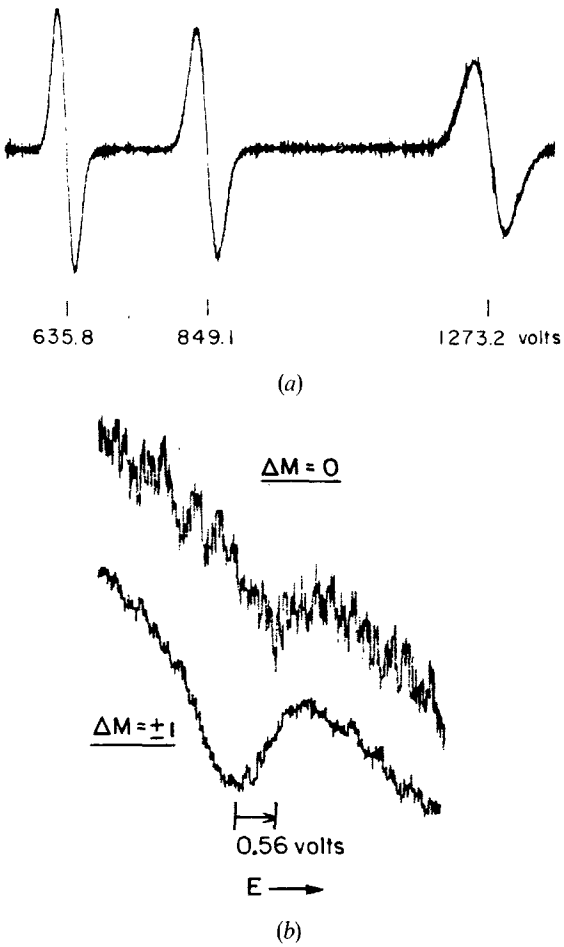


Figure 3. Laser Stark spectrum of $NH_2D$ obtained using the 10P(20) $CO_2$ laser line. (*a*) Travelling wave Doppler limited spectrum with selection rule $\Delta M = \pm 1$. The gas pressure in the cell is 50 mTorr. (*b*) Lamb dip spectrum with a gas pressure in the cell of 80 mTorr and a linewidth of $\sim 2{\cdot}9$ MHz full width at half maximum. The transitions in the upper trace are $M_J = \pm 3 \leftarrow \pm 3$, and in the lower trace $M_J = \pm 4 \leftarrow \pm 3$. (Reproduced by permission from *Physics Review Letters*, 1969, **23**, 560.)

dependence of the electric dipole moment of polar molecules. In addition the technique has been enhanced by the development of double resonance methods based on modulated $CO_2$ lasers, on microwave–infrared double resonance, on developments involving tunable laser, and on the use of low-pressure molecular beams.

## 2. Experimental methods

In laser Stark spectroscopy, fixed-frequency laser radiation is passed through a parallel plate Stark cell. At certain values of the applied electrostatic field specific electric field components of molecular vibration–rotation, or pure rotation, transition in the absorbing gas are brought into resonance with the laser frequency, giving rise to an electric resonance spectrum.

The frequencies of many of the gas lasers have been determined very accurately as part of the programme to determine the velocity of light. The most extensive data are for $CO_2$ (Petersen *et al.* 1984), isotopic variations of $CO_2$ (Freed *et al.* 1980), CO and its isotopic forms (Dale *et al.* 1979) and $N_2O$ (Whitford *et al.* 1975). All the measurements of Stark shifts are therefore made relative to secondary frequency standards. It is for this reason that laser Stark spectroscopy suffers less from calibration problems than many of the methods which employ tunable lasers.

In microwave spectroscopy it is conventional to use a waveguide Stark cell in which the electric vectors of the static electric field and of the radiation field are parallel, giving rise to the selection rule $\Delta M_J = 0$. However, with higher frequency sources a parallel plate Stark cell is used in which free space propagation of the short wavelength infrared radiation occurs. This makes it easy, and also desirable, to use both perpendicular and parallel polarisation configurations in the electric resonance experiments, so that transitions corresponding to both $\Delta M_J = 0$ and $\Delta M_J = \pm 1$ selection rules are observed.

Since the resonance method relies on the use of an electric field for tuning, it is necessary both to generate high uniform fields and to study molecules with appreciable Stark tuning coefficients. In order to generate high electric fields, which may approach $90\,kV\,cm^{-1}$, narrow electrode spacings of from 1 to 4 mm are commonly used. With such narrow gaps the plates must be flat to one or two fringes of visible light, and must be held accurately parallel. It has been found that slight warps in the plates can be corrected by tight clamping on to precision quartz spacers, and most cells incorporate this facility. Two types of plates have been used, metallized glass (Sakurai *et al.* 1967) and metal plates (Shimizu 1970 a, b). Glass plates can be made very flat but they are easily damaged by fracture or by removal of the metal coating by flash-over. The metal plates, particularly those of lapped stainless steel, are robust but need careful lapping. They can also cause problems associated with their residual magnetism when used with paramagnetic species.



The plate spacing is not usually measured directly using gauge block methods; it is derived from measuring the Stark effect in a molecule whose ground-state dipole moment has been accurately determined by molecular beam electric resonance. The molecules which are usually used for this purpose are $CH_3F$ (Wofsy *et al.* 1971, Marshall and Muenter 1980), $NH_3$ (Marshall and Muenter 1981) and OCS (Reinartz and Dymanus 1974).

The gas pressure used must also be restricted to the low-pressure region below 100 mTorr (Sakurai *et al.* 1967). A useful rule of thumb is that a potential difference of 3000 V may be sustained without electrical breakdown across any gas at a pressure of 10 mTorr and below. The Paschen curve for a particular gas can then be used to extrapolate to a different pressure/voltage regime. It should be noted that the minimum in a Paschen curve occurs at ca. 1 Torr pressure, and hence that very restricted Stark tuning is available unless much lower or much higher pressures are used. Some experiments have been carried out on Stark-modulated electronic spectra at high gas pressures, using $SF_6$ as a gaseous electrical insulator (Buckingham and Ramsay 1965, Bridge *et al.* 1967). However, the resultant pressure broadening is such that the linewidths are very much greater than the Doppler width of the infrared transitions, and also the use of saturation techniques is precluded by the rapid relaxation processes caused by the high frequency of collisions.

The detectors used are quantum-limited liquid nitrogen cooled devices, PbSnTe or CdHgTe in the 10 $\mu$m region, and InSb or Au doped Ge in the 5 $\mu$m region. In the far infrared Golay cells have been used, but in order to achieve a better signal-to-noise

ratio it is necessary to use detectors cooled by liquid helium. In order to get above the principal noise region of the electric discharge lasers used in the 5 and 10 $\mu$m regions, and as pumps for the FIR lasers, it is necessary to use electric field modulation frequencies in the range from 5 to 100 kHz.

Although the initial experiments used a single-pass absorption cell outside the laser cavity, the more recent studies have generally used either an intracavity cell or a multiple-pass cell of the type described by Shimizu (1975 c). The use of these cells leads not only to an enhanced sensitivity because of the increased path length, but also to resolution enhancement. This is due to the fact that most vibration–rotation transitions can be power saturated by the standing-wave field, leading to the production of sub-Doppler 'Lamb dips'.

This type of resolution enhancement is possible because in the mid-infrared the absorption lines are predominantly heterogeneously broadened by the Doppler effect. The effects of the saturating field are then confined to a narrow frequency region, which is centred on the velocity component of the group of molecules whose absorption is Doppler shifted into resonance (Duxbury 1983). This produces a 'hole' in the population of the lower state and a 'spike' in the population of the upper state; this effect is shown schematically in figure 4. In a standing-wave field two holes are burned, one on either side of line centre, corresponding to the two groups of molecules whose



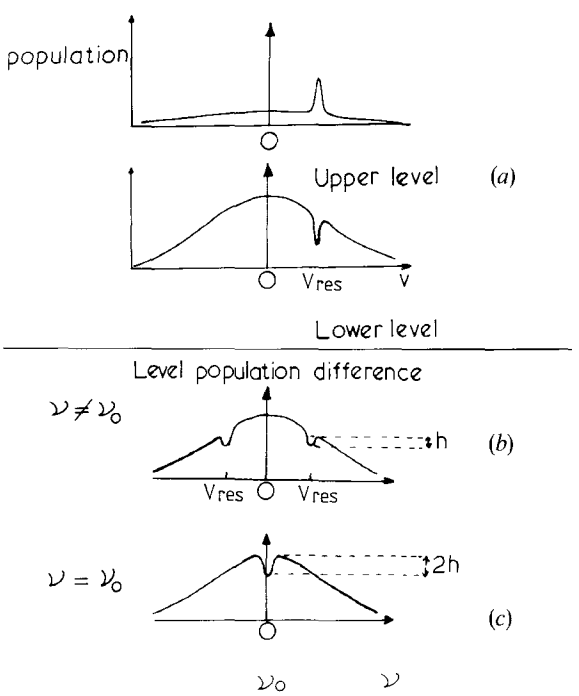


Figure 4. Saturation of an inhomogeneously broadened line. (*a*) Changes in particle velocity distribution under the action of a laser of frequency $\nu$. The $z$ component of velocity of the particles interacting with the light wave is $v_{res} = c(\nu - \nu_0)/\nu_0$. A Bennett hole is generated in the lower level and a population peak in the upper level. (*b*) Changes in population difference induced by a standing wave off resonance, $\nu \neq \nu_0$. (*c*) On resonance, $\nu = \nu_0$, a double saturation effect is observed at line centre, the Lamb dip.

absorption can then be shifted into resonance. At line centre the holes coalesce. This corresponds to one group of molecules with zero velocity component along the direction of the standing wave-field interacting with both running wave components. This double saturation results in a sharp dip in the absorption coefficient at line centre, the 'Lamb dip'. The width of this feature is governed mainly by pressure broadening, and hence it is very much narrower than the Doppler width.

Schematic diagrams of the principal types of saturation spectrometers are given in figure 5. The main disadvantage of the majority of the intracavity systems is that plate spacings of 3 to 4 mm are needed so that the gap is comparable with the spot size of a mid-infrared laser with a nearly hemispherical cavity. This means that either the fields are limited to ca. 30 kV cm$^{-1}$, or that very low gas-pressure must be used. For 10 $\mu$m operation it is possbile to use narrower plate spacings—and hence higher fields—by



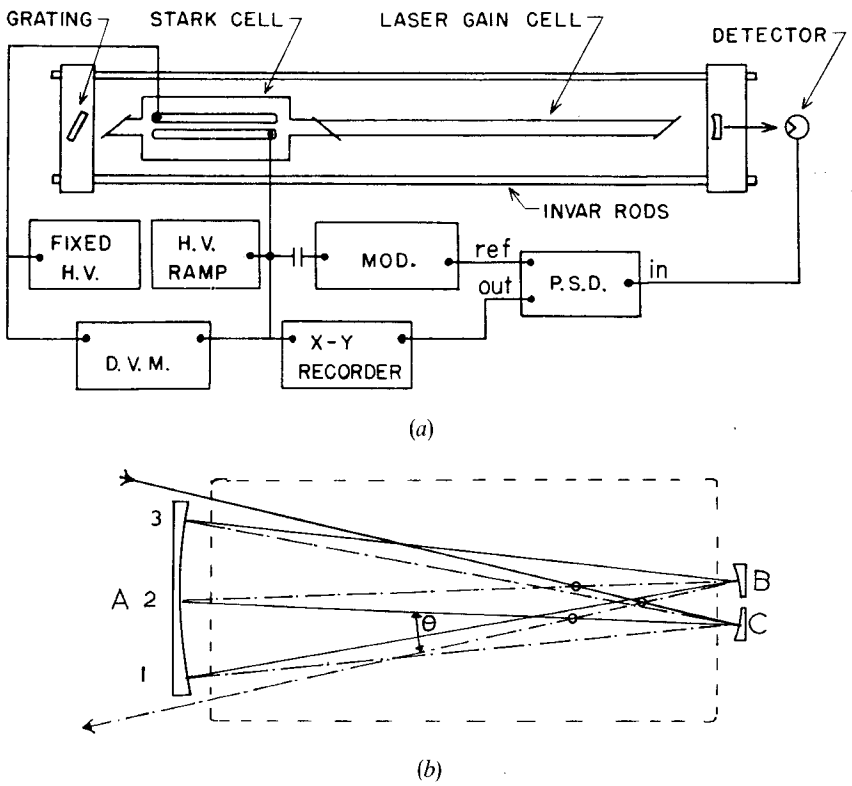


Figure 5. (*a*) Schematic diagram of an intracavity laser Stark spectrometer. PSD stands for phase sensitive detector, DVM for digital voltmeter, HV for high voltage, and MOD for modulation source. (Reproduced by permission from *Journal of Chemical Physics*, 1977, **66**, 1217.) (*b*) Mirror configuration of a cross-over White's cell of the Shimizu type with $N=4$. The solid lines show beams propagating from left to right, and the broken lines from right to left. The circles are the crossing points between solid and broken lines. The angle $\theta$ represents the finite crossing angle of the beams. The Stark electrodes are parallel to the plane of the paper, and occupy the area shown by the broken line rectangle. (Reproduced by permission from *Journal of Molecular Spectroscopy*, 1978, **69**, 239.)

incorporating additional intracavity lenses to optically match the cell into the cavity (Lahaye *et al.* 1985). This method results in rather large internal losses in the system, and hence a long gain section is necessary in the laser. The other disadvantage is that the power of the laser must be optimized for each line since the gas has a very nonlinear effect on the laser oscillations. These effects are less marked in the 5 $\mu$m region, where the gain of the CO laser lines used is comparable with the absorption in the gas cell, and where the diffraction losses imposed by the cell spacing are less important. The advantages of the use of the intracavity cell stem from the amplification of weak signals due to the non-linear gain of the laser, and from the elimination of the crossing angle between the forward and backward beams of the multiple-pass cell, resulting in higher resolution.

The amplitude of the electric field modulation used to detect the signals is usually small compared to the equivalent electric field linewidth of the transitions. The most common modulation waveform is sinusoidal (Freund *et al.* 1974), although square-wave modulation has also been used (Johns and McKellar 1975). If the modulation amplitude is much smaller than the linewidth, detection at the fundamental modulation frequency results in a first derivative lineshape as in analogous E.S.R. spectra. In order to remove the effects of sloping baselines produced by transitions with a slow Stark effect, it is common to use detection at either the second or third harmonic of the modulation frequency. Second-harmonic detection produces a second-derivative signal, resembling a sharpened absorption line but with negative side lobes. Third-harmonic detection produces a third-derivative signal which resembles a sharpened first derivative, but which again possesses side lobes. These lineshapes are illustrated in figure 6. Second and third harmonic detection are particularly useful for the observation of narrow saturation features free from background effects.



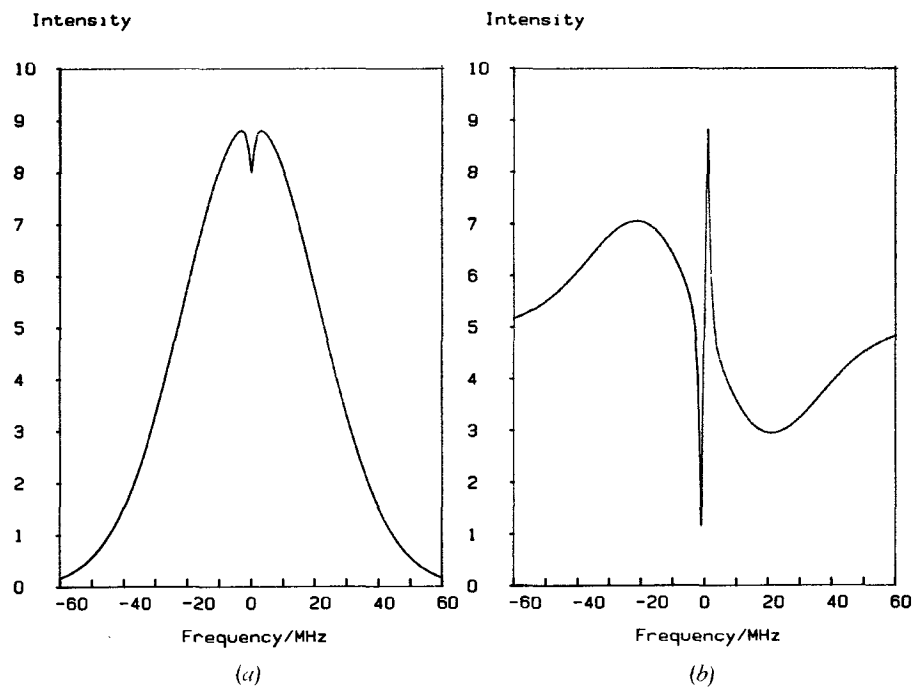

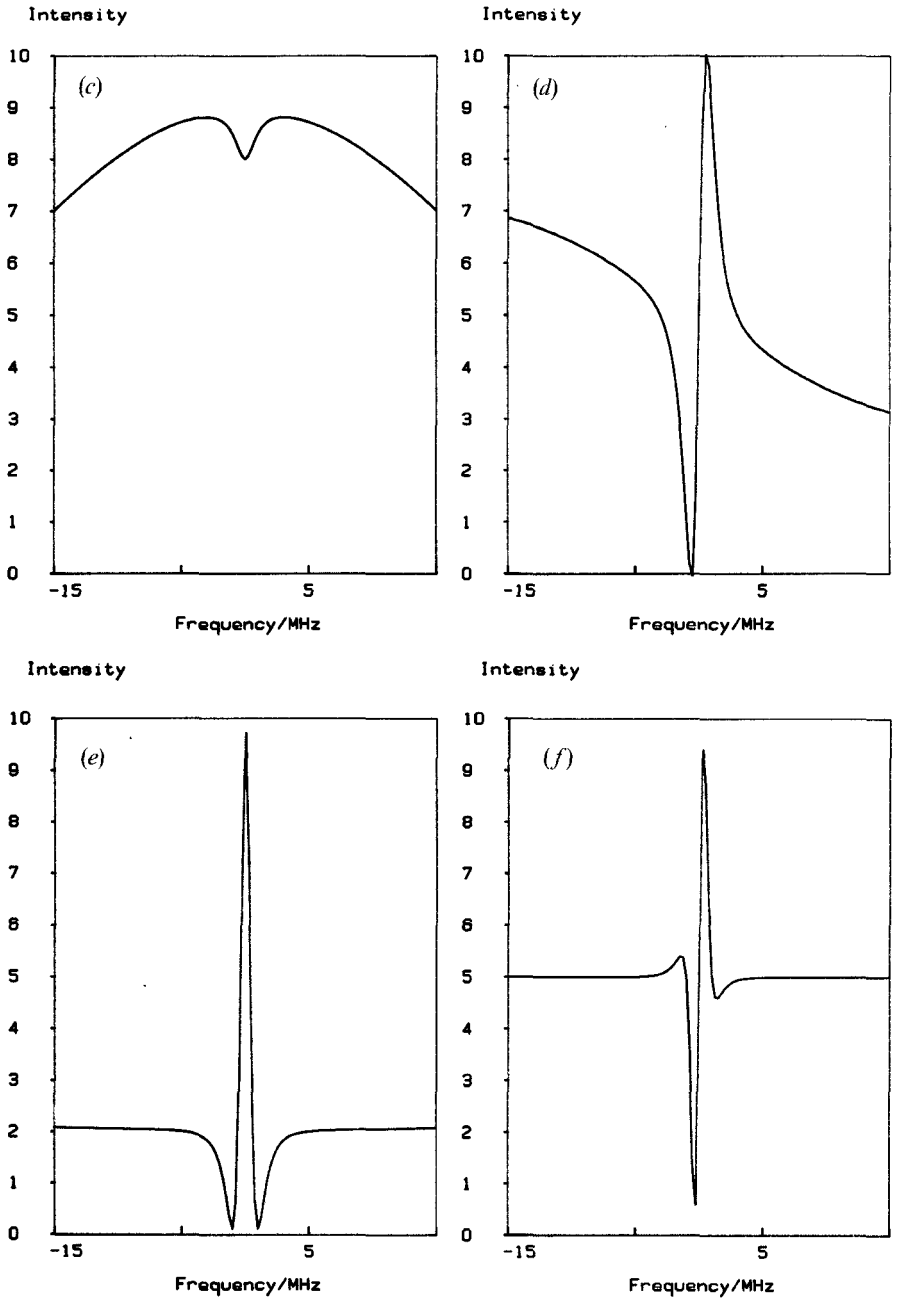


Figure 6. Line-shapes which occur when detecting at harmonics of the modulation frequency when small-amplitude field modulation is used. (*a*) 120 MHz scan of a partially saturated Doppler-broadened line showing the Lamb dip. (*b*) 120 MHz scan with fundamental, first-derivative detection. The gain is increased by a factor of eight from (*a*). (*c*) 30 MHz scan of the absorption line about the Lamb dip. (*d*) 30 MHz scan with first-derivative detection, as (*b*). (*e*) 30 MHz scan with second-harmonic, second-derivative detection. The gain is increased by a factor of four from (*a*). (*f*) 30 MHz scan with third harmonic, third derivative, detection. The gain is identical to that in (*a*).

$$\alpha(\nu)=\left\{0{\cdot}9-0{\cdot}1\left(\frac{1}{1+x^2/\gamma^2}\right)\right\}\exp\{-(x/\delta)^2\}$$

where $\gamma$, the half-width for homogeneous broadening, is 1 MHz, and $\delta$, the half-width parameter for Doppler broadening, is 30 MHz. $x=\nu-\nu_0$.

An alternative to saturation spectrometers for high-resolution studies is the use of molecular-beam systems. This has been demonstrated recently by the observation of the spectrum of $CH_3F$ using a supersonic molecular beam and bolometric detection (Douketis and Gough 1983). One of the resultant Stark patterns is compared in figure 7 with the same spectrum recorded using the Lamb dip method. The effects of the jet cooling can be seen on the relative intensities of the two series of $M$ components in the two spectra.

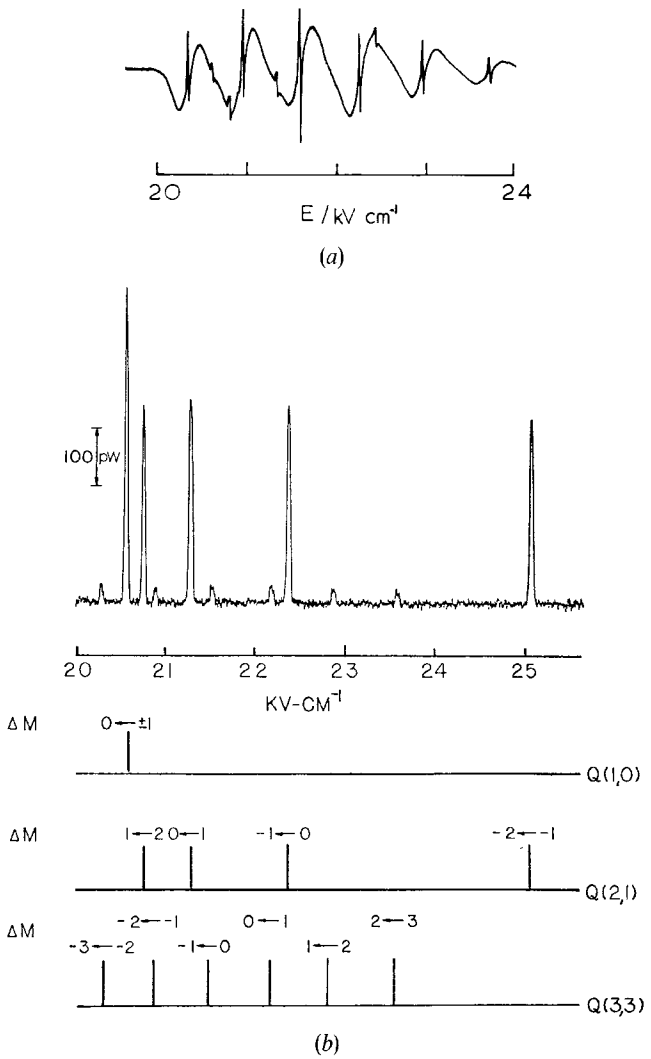


Figure 7. A portion of the laser Stark spectrum of methyl fluoride investigated by Lamb dip and by molecular-beam bolometric spectroscopy, using the 9P(18) line of a $CO_2$ laser. (*a*) Lamb dip spectrum obtained with a gas pressure of 5 mTorr at a temperature of ca. 300 K. (*b*) Low-temperature bolometric spectrum of $CH_3F$ in He, expanded through a 35 $\mu$m nozzle ($P_0D_n = 3{\cdot}3$ Torr cm). The vertical scale has been converted to watts detected by the bolometer. (Reproduced by permission from *Journal of Molecular Spectroscopy*, 1983, **101**, 325.) Note the very different intensity ratios of the $^QQ(3, 3)$ and the $^QQ(2, 1)$ transitions, and the 'forbidden' $^QQ(1, 0)$ transition, in the high and low-temperature spectra.

One of the problems of laser Stark spectroscopy is the conversion from a scale based on electric field to one based on frequency. This problem arises since there are two unknowns, the molecular dipole moment and the mismatch between the absorption line and the laser line. One solution is to use dipole measured by another technique, such as microwave spectroscopy, or to use another method, such as Fourier transform spectroscopy, to give the location of some of the absorption lines. There are however two possible techniques for measuring the Stark tuning rate directly. The first of these, due to Rackley and Butcher (1980), involves the superimposition of a strong radio-frequency field on the molecules in the cell. This produces a high-frequency Stark (Autler–Townes 1955) effect and leads to the generation of multiple sidebands in the spectra. The spacing of the sidebands in terms of electric field can then be directly related to the radio-frequency employed. The second, due to Bedwell and Duxbury (1979) uses acoustic-optic modulation of the $CO_2$ laser itself to generate a known difference frequency between the two beams propagating through the cell. In this case the sideband patterns are simpler, and the frequency–field calibration may be readily accomplished.

The absolute accuracy of the measurements also depends on the frequency stabilization of the gas lasers used. In many of the experiments in the 5 and 10 $\mu$m regions the lasers are locked to the peak of the gain curve, resulting in a possible error of ca. $\pm 3$ MHz. In the 10 $\mu$m region the $CO_2$ lasers can be accurately locked to narrow saturation features in the sidelight from a low-pressure $CO_2$ fluorescent cell (Freed and Javan 1970, Lahaye *et al.* 1985). In this way the full accuracy of the tabulated $CO_2$ line positions may be used (Petersen *et al.* 1984, Freed *et al.* 1980).



## 3. Assignment of laser Stark spectra

The electric resonance transitions seen in the laser spectra of the $\nu_3$ band of $CH_3F$ form a useful vehicle for discussing typical laser Stark patterns. The 9 $\mu$m $P(18)$ line of the $CO_2$ laser lies very close to the $\nu_3$ band origin (Freund *et al.* 1974). In perpendicular polarization several low J $^qQ$ transitions can be observed. The spectrum, displayed in figure 8, consists of a set of $^qQ$ transitions ($^{\Delta K}\Delta_J$) which are brought into resonance at differing values of the static electric field. The origin of these patterns is shown in the energy level diagram of figure 9. It can be seen that if the dipole moment of the molecule were the same in the two vibrational states and if the Stark tuning approximates to first order, all of the $M_J$ components of a particular vibration–rotation will be degenerate. Since the Stark effect in many of the rovibrational transitions of $CH_3F$ us nearly first order, the centre of the patterns is determined by the average value of the dipole moment in the two states, and the spread of the pattern by the difference. The number of components is given by $2J$, and hence gives the $J$ value of the transition. It should be noted that if the conventional microwave spectroscopic convention of parallel polarization is used these resonances are seen only at very high values of the electric field. In parallel polarization the transitions tune at a rate proportional to the dipole moment difference, ca. 0·05 D, rather than at a rate proportional to the dipole moment of 1·86 D, as is the case in perpendicular polarization. The rather asymmetric pattern of the $^qQ(3, 2)$ transition shows that at high values of the Stark field second and higher-order effects of the field may become important. This means that the usual perturbation theory treatment of the Stark effect is inadequate for transitions involving levels with low $J$ values, and that methods involving the diagonalization of truncated infinite matrices must be used in order to fit the spectra. These methods are described in more detail in section 4.

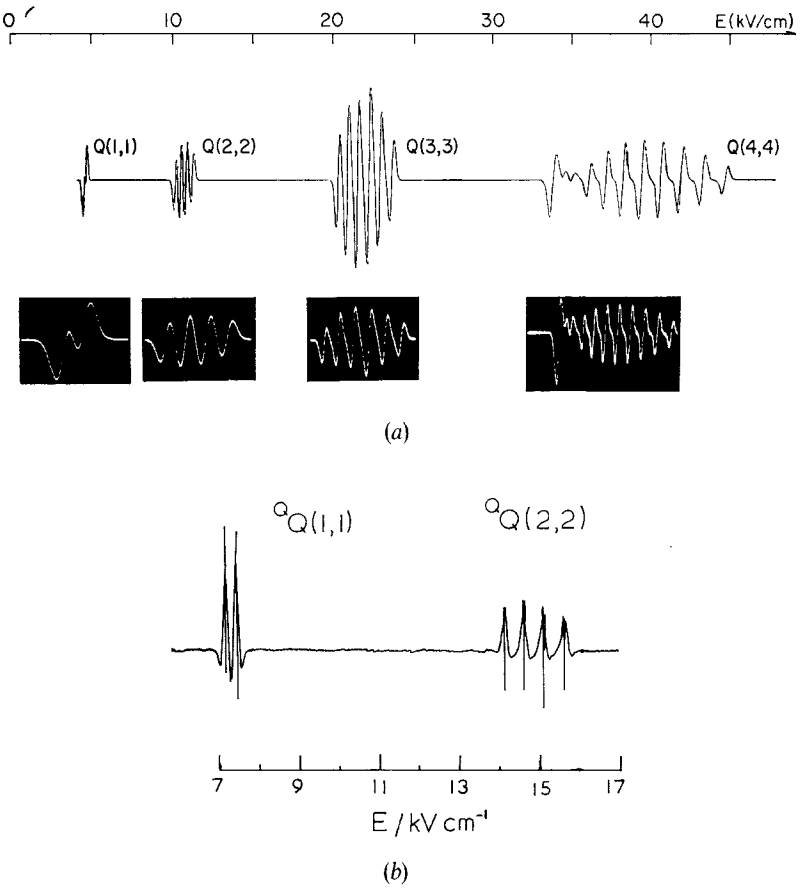


Figure 8. (*a*) Observed $\Delta M = \pm 1$ transitions for the Q-branch series of $^{12}CH_3F$. The laser line used is 9P(18) of $CO_2$. The upper trace is a computer-calculated band contour and the lower picture shows observed oscilloscope traces. The sample pressure was ca. 5 mTorr and the time constant for detection was 10 ms. (Reproduced by permission from *Journal of Molecular Spectroscopy*, 1974, **52,** 38.) (*b*) Q-branch series of $^{12}CH_3F$ with Lamb dip resolution using the 9P(44) line of $^{12}C^{18}O_2$. The time constant was 100 ms.

P and R branch transitions of parallel bands do not show the same compact structure as Q branches, and the overlapping structure of the transitions associated with the many $K$ components of high $J$ transitions is sometimes difficult to unravel. In this instance it is often useful to obtain the spectra of these transitions in parallel polarization where the patterns are simpler.

Perpendicular bands of symmetric or near-symmetric rotors exhibit more complicated Stark patterns than those of parallel bands. However, owing to the frequent proximity of vibrational states between which strong Coriolis coupling can occur, many of the spectra of quite small molecules such as $CH_2NH$ (Duxbury and Le Lerre 1984) can show very complicated electric-field spectra. In such spectra the most obvious transitions are frequently the $^{r}Q$ or $^{p}Q$ transitions seen in parallel polarization. In such resonance spectra the intensities of the successive $M_J$ components are

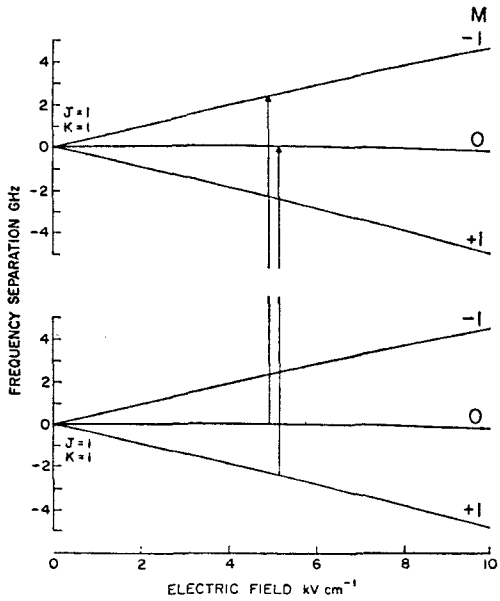


Figure 9. Stark energy-level diagram for the Q(1, 1) transition of $^{12}CH_3F$ with $\Delta M = \pm 1$. Since the Stark shifts of the excited and ground states are very similar, the splitting of the Q(1, 1) resonance indicated in figure 8 is caused by the small difference between the dipole moments in the upper and lower states of $CH_3F$. (Reproduced by permission from *Journal of Molecular Spectroscopy*, 1974, **52**, 38.)



proportional to $M^2$, as shown in figure 10. Simple formulae similar to those described by Hougen (1975) for L.M.R. spectra are useful in the initial analysis of Stark spectra (Duxbury and Freund 1977). If the dipole moment change is small, we can set $\mu' \sim \mu''$, and for low to medium-strength electric fields we can assume a first-order Stark effect. The shifts of the $^rQ$ resonances in parallel polarization are then given by $\mu E M_J/J(J+1)$, with the first member having $M_J = J$. The perpendicular $M_J = +1$ resonances are shifted by $\mu E(M_J + K + 1)/J(J+1)$, where $M_J + 1 = J$ for the first member. The ratio of the voltages of the first members of the patterns, $V_{\|}/V_{\perp} = (J+K)/J$. Since $J$ can be determined by following several members of the set of parallel polarization resonances, both $J$ and $K$ can be determined in this way.

If the molecular spectra being studied belong to a near-prolate asymmetric rotor, many of the signals observed are almost identical to those that would be produced if the molecule were a symmetric rotor. This similarity arises from the fact that the asymmetry splitting of energy levels with $K_a \geqslant 3$ is usually very small and hence in molecules such as $H_2CO$, where the permanent electric dipole moment lies along the near-prolate top a-axis, the majority of the spectra resemble those of the prototype $CH_3F$. Differences arise for the lowest $J$ and $K$ transitions, where the effects of the asymmetry splitting are evident. The effects of the lower symmetry on the nuclear spin statistics are also shown by the intensity of ratios of transitions with $K_a''$ even and $K_a''$ odd, which are different from those produced in a symmetric rotor. The change-over from asymmetric to symmetric rotor patterns is easily seen in the spectrum of the Q branch region of the $\nu_2$ band of formaldehyde (Johns and McKellar 1973) shown in figure 11.

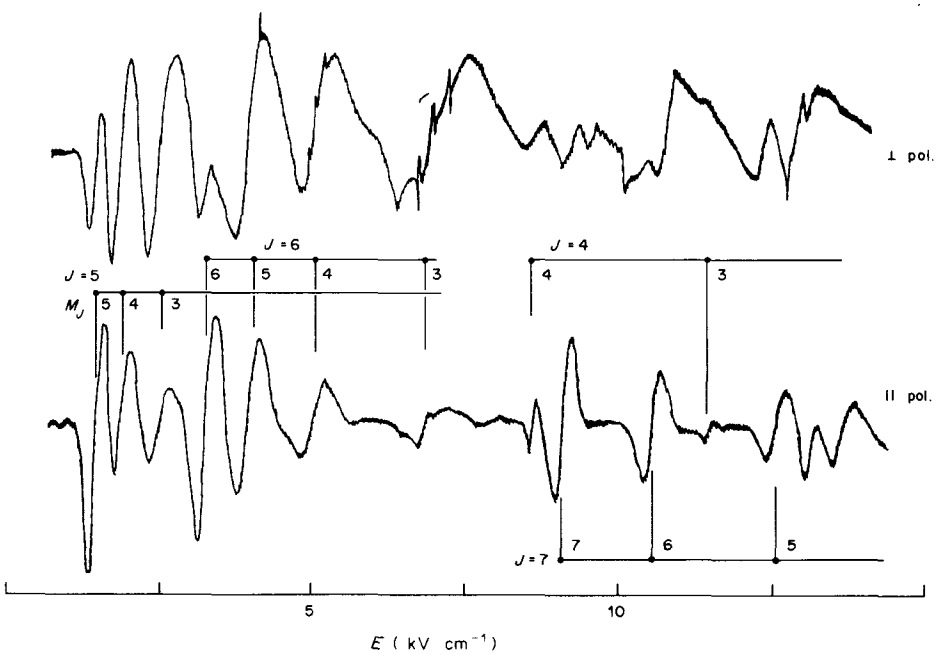


Figure 10. The laser Stark spectrum of the $^rQ(J,2)$ transitions of the $v_7$ band of $CH_2NH$ in perpendicular and parallel polarization using the 9R(10) line of a $CO_2$ laser. The different series of resonances are easily differentiated in the parallel polarization spectra. (Reproduced by permission from *Infrared Physics*, 1984, **24**, 270, Pergamon Press.)

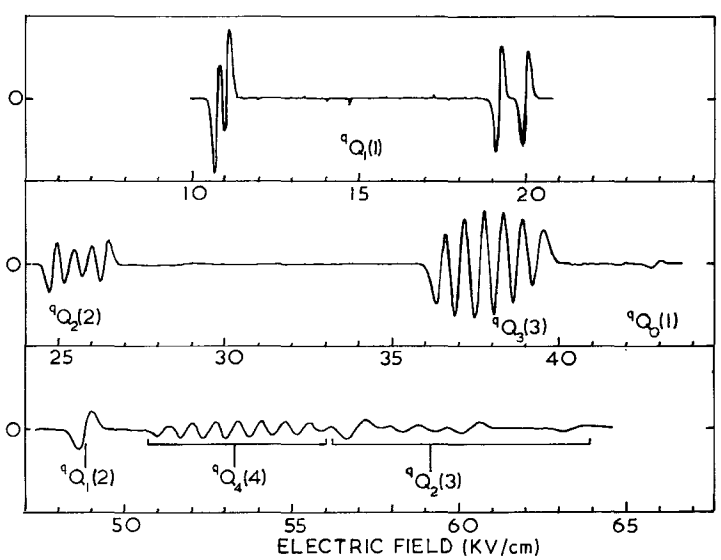


Figure 11. Laser Stark spectrum of the $^qQ$ branches of the $v_2$ band of $H_2CO$ obtained with the 14–13 P(16) line of the CO laser at 1746·307 $cm^{-1}$. The selection rule is $\Delta M = \pm 1$. Note the change from asymmetric to symmetric rotor patterns as $J$ and $K_a$ increase. (Reproduced by permission from *Journal of Molecular Spectroscopy*, 1973, **48**, 364.)

In the spectra of molecules with both a- and b-axis components of the dipole moment, such as HNO (Johns and McKellar 1977 b), further departures from the symmetric-top model become apparent. Some molecules, such as $CH_2F_2$, possess only a b-axis component of the permanent dipole moment, and hence exhibit purely asymmetric rotor patterns (Kawaguchi and Tanaka 1977).

Since the electric field mixes energy levels of opposite parity, the application of high fields leads to a breakdown of the usual electric-dipole selection rules for the transitions. As the Stark perturbation is often greater than the separation of the asymmetry doublets, the mixing produced by the electric field is sufficient to cause the field-induced transitions to possess a similar intensity to the 'normally' allowed transitions. A consequence of this is that in studies of perpendicular bands of asymmetric rotors it is frequently impossible to deduce, purely from the evidence afforded by the analyses of the laser Stark spectra, whether the vibrational transition moment lies along the b or c molecular axis. A more complete discussion of the consequences of this ambiguity is given in a recent *Faraday Discussion* (Mills *et al.* 1981).

Many of the complications associated with the analysis of L.M.R. spectra are associated with the effects of spin uncoupling, the Paschen–Beck effect. In most of the closed-shell molecules studies by laser Stark spectroscopy this type of effect cannot occur. However, there are two types of system where the 'electric' Paschen–Back effect has been observed: in the spectra of paramagnetic species such as HCO (Landsberg *et al.* 1977), and where the molecule being studied possess nuclei with a large electric quadrupole moment, as for example iodine in $CD_3I$ (Kawaguchi *et al.* 1977, Caldow *et al.* 1978). In the first case, HCO, the application of a large electrostatic field produces a decoupling of $N$ and $S$, so that the low-field coupling scheme of $|NJSKM_J\rangle$ is changed to that of $|NKSM_NM_S\rangle$ at high field. In the second case, exemplified by $CD_3I$ which contains a single quadrupolar nucleus on axis, the low-field coupling scheme of $|JKFM_F\rangle$ changes to that of $|JKM_JIM_I\rangle$ at high values of the electric field. An example of the effects of this type of uncoupling will be given in the section on 'Level-crossing Spectra'.

The linewidths observed in the spectra often provide clues to the assignment of spectra. If the Stark shifts are approximately first order, the apparent widths of the lines in terms of electric field are related to the Doppler width by the relationship

$$\Delta V/V = \Delta\nu_D/(\nu_{laser} - \nu_0) \tag{1}$$

where $\Delta V$ is the width of the resonance, and $V$ is the central voltage. $\Delta\nu_D$ is the width between the points of maximum slope, and $(\nu_{laser} - \nu_0)$ is the frequency off-set between the laser and zero-field line. This relationship was particularly useful in the analysis of the spectrum of an unstable species such as HNO or $H_2CS$, where the conventional gas-phase spectrum has not been obtained at the time of the original analysis, and where the band origins were obtained from matrix isolation data at low resolution.

## 4. The calculation of the high-field Stark effect

Since the mismatch between the laser lines and the zero-field molecular absorption line frequencies is usually several thousand MHz, large Stark shifts are needed in order to tune the $M$ components of a transition into resonance. Since these shifts are a

sizeable fraction of the spacing of the rotational energy levels, the perturbation treatment of the Stark effect is not usually a good approximation. Therefore in most cases the Stark shifts are calculated by diagonalizing the matrix of

$$H = H_{\text{rot}} - \boldsymbol{\mu} \cdot \mathbf{E} \tag{2}$$

This is an infinite matrix and must therefore be truncated at some value of $\Delta J$ greater than the $J$ value of interest. The value of $\Delta J = J_{\text{trunc}} - J$ necessarily depends on whether a high or low $J$ value is involved; $\Delta J = 2$ or 3 is often sufficient. In the most common approximation a different effective dipole moment is used for each vibrational state. The simplest application of this method is to a symmetric rotor in an $A_1$ vibrational state (Freund *et al.* 1974). The matrix elements for overall rotation and Stark interaction are given in table 1. It can be seen that the resulting matrix is tridiagonal, and hence that the eigenvalues can be obtained rapidly using the many numerical methods available for systems of bandwidth three.

Table 1. Matrix elements of the effective Hamiltonian, $H = H_{\text{rot}} - \boldsymbol{\mu} \cdot \mathbf{E}$, of a symmetric rotor in a non-degenerate vibrational state.

*Diagonal elements*

$$\langle J, K, M|H|J, K, M\rangle = BJ(J+1) + (A-B)K^2 - D_K K^4 - D_{JK} K^2\{J(J+1\} - D_J J^2(J+1)^2 - \mu\varepsilon MK/(J(J+1))$$

*Off-diagonal elements*

$$\langle J, K, M|H|J-1, K, M\rangle = -\frac{1}{J}\left[\frac{(J^2-K^2)(J^2-M^2)}{(2J-1)(2J+1)}\right]^{1/2}\mu\varepsilon$$

where $A$ and $B$ are rotational constants in $\text{cm}^{-1}$, $\varepsilon = 0{\cdot}016793E$, with $\mu$ in Debye and $E$ in kV/cm, and the $D$s are centrifugal distortion constants.

The use of this type of approach becomes a little more cumbersome for asymmetric rotor molecules in 'well isolated' vibrational states. The off-diagonal matrix elements of the rotational Hamiltonian couple states of the same $J$ values differing in $K_a$ by 2. As a result the matrices which need to be diagonalized are very much larger, and are no longer tridiagonal. If only the a-component of the permanent dipole moment is involved, the matrices may be factorized into two non-interacting blocks with $K_a$ odd and with $K_a$ even. However, if a and b components of $\mu$ occur, this factorization is no longer possible (Johns and McKellar 1977 b). The matrix elements for rotation and a- and b-axis Stark interaction are given in table 2.

In many of the molecules that have been studied recently, there are several closely spaced vibrational states which are coupled by a strong Coriolis interaction. This considerably increases the complexity of the problem of calculating the Stark interaction since the number of blocks within each truncated matrix increases by a factor of two or three, depending upon the number of interacting vibrational states. The matrix elements for this coupling are given in table 3. The presence of the electric-dipole matrix elements also destroys the basis of the factorization methods commonly used to reduce the size of the Coriolis interaction matrix in the field-free problem. It has recently been discovered (Duxbury *et al.* 1985) that in some cases an interference effect between the Coriolis and Stark matrix coupling terms can be observed. This is analogous to the intensity interference effects caused by strong Coriolis coupling between closely spaced infrared bands.

Table 2. Matrix elements of the effective Hamiltonian of a near-prolate asymmetric rotor in a type $I^l$ representation, so that the matrix elements of $\mu_a$ and $\mu_b$ are real. The energies are measured in $cm^{-1}$ units.

*Diagonal matrix elements*

$$\langle J,k,m|H|J,k,m\rangle = \bar{B}J(J+1)+(A-B)k^2-\Delta_K k^4-\Delta_{JK}k^2\{J(J+1)\} - \Delta_J J^2(J+1)^2-\mu_a\varepsilon mk/(J(J+1))$$

where $k$ and $m$ are signed quantum numbers ($K=|k|$, $M=|m|$), $k$ is to be identified with $k_a$, $\bar{B}=(B+C)/2$, $A$, $B$ and $C$ are the rotational constants in $cm^{-1}$ and the $\Delta$s are centrifugal distortion constants. $\varepsilon=0{\cdot}016793E$, with $\mu$ in Debye and $E$ in kV/cm.

*Off-diagonal rotational matrix elements*

$$\langle J,k,m|H|J,k\pm2,m\rangle = \{(B-C)/4-\delta_J J(J+1)-\delta_K(k^2+2k+2)\} \times\{(J(J+1)-k(k\pm1)\}\{J(J+1)-(k\pm1)(k\pm2)\}^{1/2}$$

where $\delta_J$ and $\delta_K$ are centrifugal distortion constants.

*Off-diagonal Stark matrix elements*

$$\langle J,k,m|H|J-1,k,m\rangle = \frac{-1}{J}\left[\frac{(J^2-k^2)(J^2-m^2)}{(2J-1)(2J+1)}\right]^{1/2}\mu_a\varepsilon$$

$$\langle J,k,m|H|J,k\pm1,m\rangle = \frac{-m}{2J(J+1)}[J(J+1)-k(k\pm1)]^{1/2}\mu_b\varepsilon$$

and

$$\langle J,k,m|H|J-1,k\pm1,m\rangle = \frac{\pm1}{J}\left[\frac{(J\pm k+1)(J\pm k+2)(J^2-m^2)}{(2J-1)(2J+1)}\right]^{1/2}\mu_b\varepsilon$$

Table 3. Matrix elements of the effective Hamiltonian for Coriolis interaction in asymmetric rotors. The phases of the wavefunctions have been chosen so that the matrix elements are real. The energies are measured in $cm^{-1}$ units.

| $C_{2v}$(e.g. $H_2CO$) | $C_s$(e.g. $CH_2NH$) | |
|---|---|---|
| $\langle v_4,J,k\|H\|v_6,J,k\rangle$ | $\langle v_7,J,k\|H\|v_9,J,k\rangle$ | $\zeta^a k$ |
| $\langle v_4,J,k\|H\|v_3,J,k\pm1\rangle$ | $\langle v_7,J,k\|H\|v_9,J,k\pm1\rangle$ | $\frac{1}{2}\zeta^b F(J,k)$ |
| $\langle v_6,J,k\|H\|v_9,J,k\pm1\rangle$ | $\langle v_7,J,k\|H\|v_6,J,k\pm1\rangle$ | $\pm\frac{1}{2}\zeta^c F(J,k)$ |

where

$$F(J,k)=\{J(J+1)-k(k\pm1)\}^{1/2},\quad K_a=|k|$$

and

$$\zeta^a(H_2CO)=\zeta^a_{64}\approx A[(\nu_6/\nu_4)^{1/2}+(\nu_4/\nu_6)^{1/2}]\zeta^a_{64}$$

and

$$\zeta^a(CH_2NH)=\zeta^a_{64}\approx A[(\nu_6/\nu_4)^{1/2}+(\nu_4/\nu_6)^{1/2}]\zeta^a_{64}$$

etc.

Since the Stark shifts are large and the resolution is very high, the variation of the dipole moment with vibrational state can be determined very accurately. In some molecules, particularly those with small induced dipole moments or those which are very non-rigid, a significant rotational variation may also be observed. Finally, if the

molecule contains $\pi$ electrons, as for example $CO_2$ or OCS, the variation of the electric polarizability with vibrational state must also be included in the calculation.

The variation of the dipole moment of a molecule with its vibration–rotation state is associated with the changes which occur in the electronic charge distribution when the nuclear frame is distorted from its equilibrium geometry. The formal treatment of these effects is similar to that applied to vibration–rotation interaction, where the vibrational and rotational distortion effects are observed via the vibrational dependence of the rotation constants and the occurrence of centrifugal distortion effects.

### 4.1. *Vibrational effects*

The dipole moment of a polyatomic molecule may be expanded as a power series in the vibrational quantum numbers, and to first order in $v$ may be written as (Toyama *et al.* 1964)

$$\mu = \mu_e + \sum_s \delta\mu_s v_s \tag{3}$$

where $\mu_e$ is the equilibrium dipole moment and $v_s$ is the vibrational quantum number of the $s$th normal code. Two terms contribute to $\delta\mu_s$, one involving first derivatives of the dipole moment with respect to changes in the vibrational coordinates, and one involving the second derivative with respect to the $s$th coordinate. For example, for the $\nu_3$ vibration of $CH_3F$, the CF stretching vibration, $\delta\mu_3$ takes the form (Freund *et al.* 1974)

$$\delta\mu_3 = -\left[\frac{k_{133}}{\nu_1}\left(\frac{\partial\mu}{\partial q_1}\right) + \frac{k_{233}}{\nu_2}\left(\frac{\partial\mu}{\partial q_2}\right) + \frac{3k_{333}}{\nu_3}\left(\frac{\partial\mu}{\partial q_3}\right) + \frac{1}{2}\left(\frac{\partial^2\mu}{\partial q_3^2}\right)\right] \tag{4}$$

where $\nu_3$ and $k_{333}$ etc. are the vibration frequencies and cubic anharmonic force constants and $q_s$ is the $s$th normal coordinate (in dimensionless units). It should be noted that the sum includes the dipole moment derivatives only for the totally symmetric vibrations in the case of $C_{3v}$ molecules such as $CH_3F$, and for the in-plane vibrations in planar $C_{2v}$ molecules such as $H_2CO$.

A number of problems arise in the comparison of the experimentally determined dipole moment variation with those expected on the basis of the theory presented above. In very few molecules is the anharmonic force field well determined (Robiette and Duncan 1983), nor is the absolute sign of the $\partial\mu/\partial q_3$ known in most cases, since the observable quantities are the infrared band intensities which depend upon the squares of the dipole moment derivatives. However, it is often possible, by the use of simplified models (Freund *et al.* 1974, Duxbury *et al.* 1976) and of information derived from the intensity asymmetries which occur in Coriolis coupled bands, to obtain some insight into dipole moment variation from an observed pattern.

### 4.2. *Rotational effects*

The theory of the rotational dependences of dipole moments is, in its present form, largely due to Watson (1970). The effect can most easily be visualized as caused by the centrifugal distortion affecting the molecular structure. This effect can be expressed as

$$(\delta\mu_\alpha)_{\text{cent.}} = \sum_k \left(\frac{\partial\mu_\alpha}{\partial Q_k}\right)(\delta Q_k)_{\text{cent.}} \tag{5}$$

where the $Q_k$ are the normal coordinates. In a molecule-fixed coordinate system the dipole moment can be written as

$$\mu_\alpha = \mu_\alpha^{(e)} + \sum_{\beta\gamma} \theta_\alpha^{\beta\gamma} J_\beta J_\gamma \tag{6}$$

where $J_\alpha$, the molecule-fixed components of the total angular momentum, are in units of $h$ and the coefficient of the dipole moment, $\theta_\alpha^{\beta\gamma}$, which is in units of electric dipole moment, is given by

$$\theta_\alpha^{\beta\gamma} = \theta_\alpha^{\gamma\beta} = 2\sum_k \left(\frac{B_\beta B_\gamma}{\omega_k^2}\right)\left(\frac{\partial I_{\beta\gamma}}{\partial Q_k}\right)\left(\frac{\partial \mu_\alpha}{\partial Q_k}\right)_e \tag{7}$$

where $B_\beta$ is the rotational constant for the $\beta$ axis, and $\partial I_{\beta\gamma}/\partial Q_k$ is the distortion of the $\beta\gamma$ component with the excitation of the $k$th vibrational mode, which is of frequency $\omega_k$.

Since the calculation of the Stark effect depends upon the projection of the molecule-fixed axes on to axes fixed in the laboratory (the space-fixed axes), only certain linear combinations of the $\theta$ parameters can be determined. In a $C_{3v}$ molecule there are only four independent $\theta$ parameters $\theta_\zeta^{\xi\xi}$, $\theta_\xi^{\zeta\zeta}$ and $\theta_\xi^{\xi\xi}$, where $\zeta$ is taken along the $C_3$ axis, the $\xi$ axis on a $\sigma_v$ plane, and the $\eta$ axis is perpendicular to them. The first-order Stark effect in a $C_{3v}$ molecule can be calculated using the 'effective' dipole moment

$$\mu_\zeta(J,K) = \mu_\zeta^{(0)} - \theta_\xi^{\xi\zeta} + (\theta_\xi^{\xi\xi} + 2\theta_\xi^{\xi\zeta})J(J+1) - (\theta_\zeta^{\zeta\zeta} - \theta_\xi^{\xi\xi} - 2\theta_\xi^{\xi\zeta})K^2 \tag{8}$$

### 4.3. *Torsional effects*

In molecules in which internal rotation can occur, such as methanol, the dipole moment can vary significantly with torsion–rotational state (Kivelson 1957, Johnston *et al.* 1980) due to the effects of centrifugal distortion. These effects can be incorporated into the torsion–rotation Hamiltonian by writing the dipole moment components as a power series of even order in the angular momentum and barrier terms

$$\mu_g = \mu_g^{(0)} + \mu_g^{(\gamma)} P_\gamma^2 + \mu_g^{(v)}(1-\cos 3\gamma) + \mu_g^{(k)} k^2 + \mu_g^{(k\gamma)} k P_\gamma + \mu_g^{(J)} J(J+1) + \ldots \tag{9}$$

where $g$ denotes the a or b molecular axis, $\gamma$ the angle of the internal rotation, and $P\gamma$ is the torsional angular momentum. In some circumstances this can be taken into account by using an effective a dipole moment for each level,

$$\begin{aligned}\mu_a^{\text{eff}} &= \mu_a^{(0)} + \mu_a^{(\gamma)}\langle P_\gamma^2\rangle + \mu_a^{v}\langle 1-\cos 3\gamma\rangle + \mu_a^{(k)}k^2 + \mu_a^{(k\gamma)}k\langle P_\gamma\rangle + \mu_a^{J}J(J+1) \\ &\equiv \mu_{a0} + \mu_{a1}J(J+1) + \ldots\end{aligned} \tag{10}$$

where $\langle O_P\rangle$ denotes an expectation value of a particular operator $O_P$ over the eigenfunction of that level. This approach will fail if the $\mu_b$ connections become important.

### 4.4. *The effects of the polarizability anistropy*

The effective Hamiltonian for this effect in an asymmetric top molecule is

$$H_\alpha = -(\tfrac{1}{2})E^2\{\alpha(\Phi_{Za} - \tfrac{1}{3}) + \beta(\Phi_{Zb}^2 - \Phi_{Zc}^2)\} \tag{11}$$

where

$$\alpha = \alpha_{aa} - (a_{bb} + \alpha_{cc})/2, \quad \beta \overline{=} (\alpha_{bb}\alpha_{cc})/2$$

and $\Phi_{Fg}$ are the direction cosine operators between the space-fixed axes $F$, and the molecule-fixed axes, $g$.

There are two contributions to the polarizability, an electronic polarizability and a vibrational one, $\alpha^{vib}$. In some examples the electronic polarizability can be obtained from Kerr effect measurements and the vibrational polarizability from the intensities of the vibrational bands (Bogaard and Orr 1975).

In most small molecules, such as $CH_3F$ and $H_2CO$, the effects of the polarizability corrections are of the order of 2 MHz for fields of 50 kV/cm and can therefore be neglected. However, in highly polarizable molecules such as $CO_2$ and OCS the polarizability anisotropy is appreciable. In linear molecules the only non-vanishing term in equation (11) is

$$\alpha = \alpha_{aa} - \alpha_{bb} = \alpha_{\parallel} - \alpha_{\perp} \tag{12}$$

where $\parallel$ and $\perp$ denote directions with respect to the molecular axis.

## 5. Other resonance methods using electric-field tuning

In addition to the original laser Stark method, there are several related methods which rely on electric-field tuning to bring about a resonance condition. Most of these methods require an almost exact coincidence between a zero-field transition in the absorbing gas and line of a $CO_2$ or CO laser. Despite this restriction these methods have been successfully applied to many molecular systems. They are in the main sub-Doppler methods in which the resonant fields are independent of the exact laser frequency. The particular methods which will be discussed are optical–optical (or infrared–infrared) double resonance (OODR), level crossing and anti-crossing, and infrared–microwave double resonance in high electric fields.

OODR and level crossing can be treated together, since in its simplest form level crossing can be regarded as the degenerate case of OODR. In OODR experiments of the type first carried out by Brewer (1970), a pair of transitions sharing a common energy level interact, with two co-propagating laser beams of different frequencies. Providing that at least one of the beams possesses sufficient power to partially saturate one velocity group, this hole can then be probed via the coupled transition, and a narrow non-linear signal will be seen. In order that such velocity matching can occur the following resonance condition must be satisfied:

$$\Omega_1 - \Omega_2 = \nu_1 - \nu_2 \quad \text{or} \quad \Omega_1 - \nu_1 = \Omega_2 - \nu_2 = \frac{v_Z \bar{\nu}}{c} \tag{13}$$

In this expression $\Omega_1 - \Omega_2 = \Delta\Omega$ is the difference between the lasers, $\nu_1 - \nu_2 = \Delta\nu$ is the difference frequency between the molecular transitions, and $\nu \sim (\nu_1 - \nu_2)/2$. The energy-level patterns for which this will occur are the 'vee' scheme of figure 12, or its inverse, the inverted 'vee'.

If two or more overlapping transitions sharing a common level become accidentally degenerate at some value of the applied electric field, a Doppler-free signal can be seen at high laser power. For two levels this is just the degenerate case of OODR. If the energy levels are associated with two transitions sharing a common level, when the energy levels become 'crossed', the two transitions become degenerate and both can be saturated at the same time. This double saturation effect can be detected by non-linear absorption of the laser light. These non-linear signals are most frequently seen at zero field when they are known as the zero-field level crossing, or Hanlé, signals. At zero field all the $M_J$ components are degenerate or 'crossed', and hence can all be saturated. Once

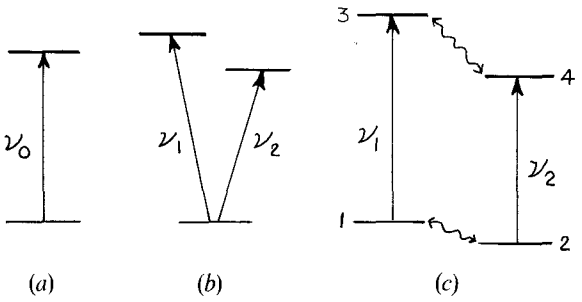


Figure 12. Schematic energy-level diagrams illustrating (*a*) Single resonance, (*b*) three-level double resonance (vee configuration), and (*c*) four-level double resonance. The wavy arrows in (*c*) represent collision-induced transitions. The three-level signals in (*b*) can be induced by one pair of counter-propagating beams of the same frequency (velocity-selected three-level signals), or by two different co-propagating beams (OODR). The four-level signals are usually velocity selected.



a finite field is applied the $M_J$ degeneracy is broken and only some of the non-degenerate components of the transition can be saturated. Thus a differential saturation signal can be seen centred on zero field. One of the first examples of this to be observed was a level crossing signal in the $\nu_3$ band of $CH_4$ (Luntz *et al.* 1969). This type of signal is seen in all cases in which OODR signals are observed, and hence it acts as a guide to lines which are suitable for study. This is because the position of the signal, whether at zero or at finite field, depends only on the degeneracy of the energy levels and not on the absolute laser frequency; thus, its position is invariant to laser drift. This property may therefore be used to discriminate level crossing signals from Lamb dips. The line-shape of the zero-field level crossing signal is rather complicated since it is associated with multiple degeneracy (Feld *et al.* 1974, Sandholm and Schwendeman 1983).

If avoided crossings between Stark sub-levels occur, sub-Doppler signals can be observed which resemble those obtained in level crossing experiments. These signals are often broader than those produced in level crossing. The theory of these signals is similar to that of non-linear level crossing (Amano and Schwendeman 1979). However, additional terms arise owing to the variation of the transition dipole matrix elements from the common level to the two interacting levels. These matrix elements have a very rapid variation in the crossing region, since at the point of nearest approach the wavefunctions of the two interacting states are almost a 50:50 mixture of the unperturbed functions. The terms in the molecular Hamiltonian responsible for the production of the weak avoided crossings are usually higher-order terms which are neglected in the standard treatment of the vibration–rotation interaction or of the Stark effect.

As we have seen above the resonance condition for which OODR signals can be observed in $\Delta\Omega = \Delta\nu$. In the earliest experiments of Brewer (1970, 1972) two very stable $CO_2$ lasers were used to generate $\Delta\Omega$. However, it was subsequently realized (Orr and Oka 1977a) that the use of a single amplitude-modulated laser removed the requirement for frequency-locking two separate lasers. It also allowed the frequency difference to be set directly as it is simply related to the frequency of the radio frequency oscillator which drives the modulator. As the sidebands move in phase with the carrier, the difference frequency is independent of the frequency drift of the laser and depends

only on the stability of the r.f. drive oscillator. Two types of modulation have been employed, electro-optic (Orr and Oka 1977 a, b, 1980) and acousto-optic (Bedwell and Duxbury 1979). The electro-optic technique was the first to be used but since acousto-optic modulators require much lower drive voltages and produce a single sideband only, they will be used in the following discussion. A block diagram of a single sideband spectrometer is shown in figure 13. By use of a half-wave plate/linear polarizer combination overall selection rules of $\Delta M_J$ (or $\Delta M_F$) $= 0, \pm 1, \pm 2$ can be produced. For the selection rule $|\Delta M_J| = 2$ either beam 1 excites transitions with $\Delta M_J = +1$ and beam 2 those with $\Delta M_J = -1$, or vice versa. The resultant resonant condition for a symmetric rotor is then:

$$\Delta\Omega = \Omega_{\text{r.f.}} = \frac{2\mu EK}{hJ(J+1)} \tag{14}$$

If the overall selection rule is $|\Delta M_J| = 1$, the resonance condition for a symmetric rotor becomes

$$\Omega_{\text{r.f.}} = \frac{\mu EK}{hJ(J+1)} \tag{15}$$

If the double resonance spectra are obtained in a multiple-pass cell, signals due to Lamb dips and three or four level-velocity-tuned double resonance signals can often be seen as well as the OODR signals. An example of this mixture of signals in methanol, including the role of polarization selection, is shown in figure 14.

If a second-order Stark effect occurs the degeneracy of the $M$ components of a double resonance signal can be broken and resolved $M$-structure seen (Orr and Oka 1977 b, Bedwell and Duxbury 1979). Similar effects can arise due to angular momentum uncoupling when a quadrupolar nucleus is present (Bedwell and Duxbury 1979).

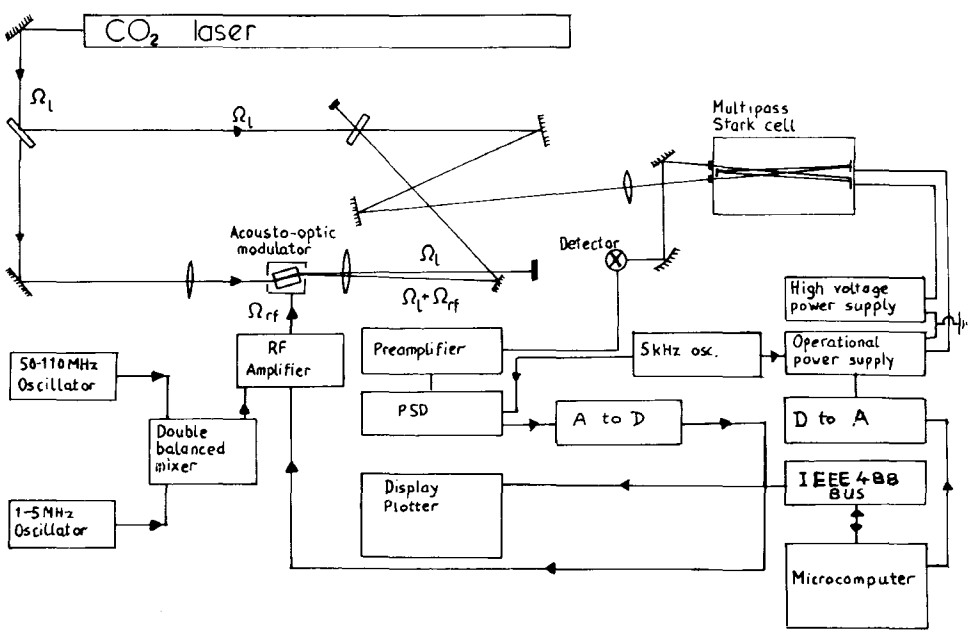


Figure 13. Block diagram of a microcomputer controlled OODR spectrometer.

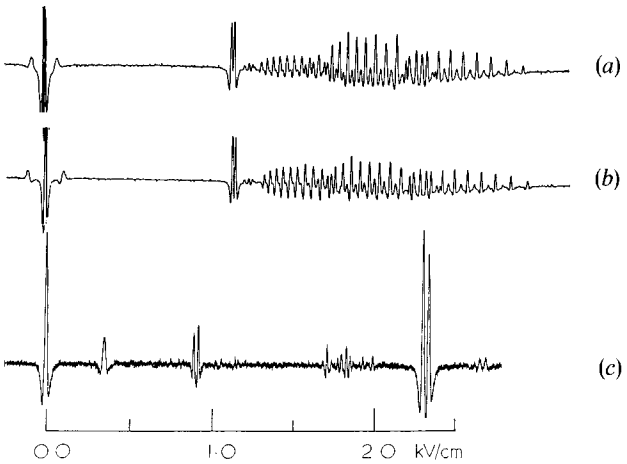


Figure 14. OODR spectra of $CH_3OH$ using the 9P(34) laser line of $CO_2$. (*a*) Two beams perpendicularly polarized, detecting in parallel polarization. (*b*) One beam perpendicular and one parallel polarized, detecting in perpendicular polarization. (*c*) As (*b*) but detecting in parallel polarization.



One of the limitations of acousto-optic modulators is that their drive frequencies are too high for the shifts which can be produced in species with small dipole moments. This limitation can be overcome by the amplitude-modulated sideband method (Duxbury and Kato 1982), in which the carrier is suppressed, and the effective frequency for double resonance is then twice that of the amplitude modulation.

An alternative method of combining radio-frequency modulation and level crossing is to apply r.f. Stark modulation to the gas being studied. Level crossings of the molecular sidebands can then occur. Although this method has been used by Luntz (1971) to measure the dipole moment in the $v_3$ state of methane, the complications associated with the presence of multiple sidebands, particularly if there is a second-order Stark effect (Macke and Legrand 1974), can lead to ambiguity in the interpretation of the data. It is for this reason that the technique has proved to be less popular than OODR.

Most of the systems in which high-field level crossing or anti-crossing signals have been observed involve a change in the angular momentum coupling scheme as the electric field is increased. These effects are seen in the $v_2$ band of $CD_3I$ in which both level crossing (Sakai and Katayama 1975, Caldow *et al.* 1978) and anti-crossing signals (Sakai and Katayama 1976) have been observed (figure 15). $CD_3I$ possesses one nucleus, iodine, which has a large electric quadrupole moment, and which lies on the principal symmetry axis. At zero field the rotational angular momentum, $J$, and the nuclear spin angular momentum, $I$, are coupled to form a resultant $F$, so that the energy levels can be characterized by $|F, M_F\rangle$. However, as the electric field strength is increased, $J$ and $I$ become more and more decoupled, so that at high field the appropriate coupling scheme is $|J, M_J\rangle\,|I, M_I\rangle$. Thus in this example the positions of the crossings or avoided crossings are determined by the ratio of the matrix element of the electric dipole moment to those of the electric quadrupole moment.

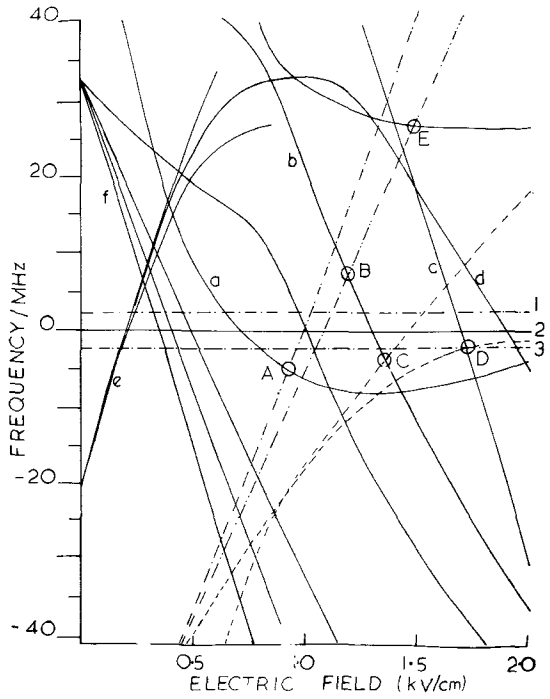


(*a*)

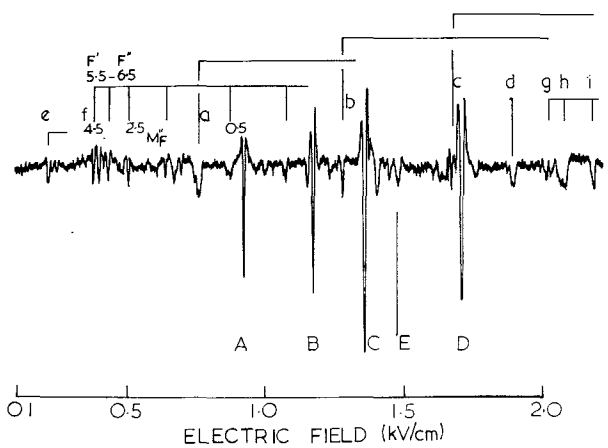


(*b*)

Figure 15. Stark effects on different $\Delta M_F = \pm 1$ transitions of the $^{Q}P(4, 1)$ vibration–rotation line of the $\nu_2$ band of $^{12}CD_3I$. (*a*) Diagram of transition frequency offset from the 10P(16) $CO_2$ laser as a function of applied electric field. The level crossing signals are labelled A to E, and the Lamb dips by a to i. Note that d gives resonances at two different Stark fields. (*b*) High-resolution spectrum obtained using a multiple-pass Stark cell. The sample pressure was about 10 mTorr and the time constant for detection was 100 ms. (Reproduced by permission from *Journal of Molecular Spectroscopy*, 1978, **62**, 242–243.)

One molecule in which an extensive range of anti-crossing signals has been observed is $POF_3$ (Amano and Schwendeman 1979). The avoided crossings occur between energy levels which differ in $|k-l|$ by $\pm 3$. Since in both level crossing and anti-crossing experiments the position of the crossing points cannot be influenced by the spectroscopist, the methods are less flexible than OODR.

Although conventional infrared-microwave spectroscopy experiments rely on accidental zero-field coincidences between lasers and molecular absorption lines, recently some high-field experiments have been carried out (Tanaka *et al.* 1976, T. Tanaka *et al.* 1982). In these experiments microwaves are injected via a horn into a multiple-pass Stark cell and the absorption of this radiation is detected via the coupled infrared transition. Since both the electric fields and the microwave frequencies can be measured very accurately, as can the zero-field microwave frequency, this provides a very accurate method of measuring the changes of molecular dipole moment with vibrational and rotational state. This method has recently been applied to the determination of the dipole moments of $H_2CO$ (K. Tanaka *et al.* 1982) and of OCS (Tanaka *et al.* 1984).

One method of combining the virtues of tunable and fixed frequency lasers in an infrared–infrared double resonance experiment was demonstrated by Weber and Terhune (1981, 1983 b). They carried out Stark tuned sub-Doppler double resonance experiments using a CO laser as a pump and a diode laser as a probe. In these experiments the electric field was used to tune certain transitions in the $v_4$ band of $NH_3$ into resonance with lines of a CO laser, and transitions involving the common lower level were probed by diode laser spectroscopy of the $v_2$ band. Complex narrow sub-Doppler features were seen including line-narrowing effects and collision-induced resonances. This method should be generally applicable to a wide range of systems with appreciable Stark effects which lie within the tuning range of $CO_2$ and CO lasers.



## 6. Stark spectroscopy of small stable molecules

Laser Stark spectroscopy and the related techniques have been used for three main purposes: as high-resolution methods of measuring the absorption spectra of low-pressure gases; as accurate methods of measuring the variation of electric dipole moment with vibrational and rotational state; and as a means of identifying the pump transitions of optically pumped submillimetre lasers.

From the earliest applications of these resonance methods it was apparent that, in most experiments, the absolute precision of dipole moment determination was little better than that achieved in the best microwave Stark modulation spectrometers. However, the laser-based spectrometers provide a direct way of measuring the small changes of dipole moment which occur on vibrational excitation. In some of the most recent high-field infrared–microwave double resonance experiments the absolute accuracy of the results approaches that of molecular beam electric resonance spectrometers.

### 6.1. *Spectroscopy and dipole moment variation of polar molecules*

The first molecule to be studied systematically by laser Stark spectroscopy was ammonia (Shimizu 1969, 1970 a, b). He discovered that a very large change in dipole moment, 0·22 D, occurred on the excitation of one quantum of the bending vibration, $v_2$, and later experimental results were interpreted as indicating a rotational dependence of the dipole moment (Shimoda *et al.* 1980). Since the inversion barrier in

ammonia is rather low—about two vibrational quanta of $v_2$—a large change in dipole moment is to be expected, since if ammonia were planar the dipole moment would be zero. As ammonia is inverting very rapidly, the 'dipole moment' of a state is really the expectation value of the dipole moment operator connecting the two components of an inversion doublet. As a result the Stark effect in the excited state is much smaller than in the ground state. The effects of this can be seen in figure 16. Above the barrier of planarity the inversion doubling eventually becomes equal to half the vibrational spacing, and hence for higher vibrational levels the vibrational spacing appears to be halved. Once the inversion doubling approaches the size of the vibrational spacing the vibrational transition moment and the 'dipole moment' become almost identical. This has been demonstrated by a recent experimental study of the $2v_2 - v_2$ band of $NH_3$ (Takami *et al.* 1979) and by the observation of the $2v_2$ band by Doppler-free two-photon spectroscopy (Bischel *et al.* 1976).

Another set of recent measurements of $NH_3$ has shown some of the pitfalls in the laser Stark approach (Weber and Terhune 1983 a). The effective dipole moments of some of the inversion–rotation levels of the $v_4$ state of ammonia were measured. $v_4$ lies close to $2v_2$, and many of the levels of the two bands are coupled by Coriolis interaction. One set of levels of the $v_4$ state is not coupled to levels of the $2v_2$ state, and the effective dipole moment of these levels is within 1% of that of the vibrational ground state. This small change is expected on the basis of the theory of vibrational changes in dipole moment given previously. The $v_4$ vibration is a perpendicular vibration so excitation of this mode should produce little effect on the average value of the dipole moment along the symmetry axis. The other levels are strongly coupled and the 'dipole moments' measured ranged from 0·793 to 1·326 D, compared with a ground-state dipole moment of 1·47 D. The laser Stark method is therefore really only suitable for studies of unperturbed states where the molecular dipole moment can be treated as almost constant. Further studies of the $v_2$ band of $^{14}NH_3$ and $^{15}NH_3$ have been made by both opto-acoustic Lamb dip (Minguzzi *et al.* 1982), intracavity Lamb dip, and OODR methods (di Lonardo *et al.* 1981, Orr and Oka 1977 b, Duxbury *et al.* 1983). In addition, sub-Doppler spectra have been obtained of $ND_3$ (di Lonardo and Trombetti 1981) and $NH_2D$ (Rackley and Butcher 1980). Spectra have also been obtained of the phosphorus and arsenic analogues, $PH_3$ (Shimizu 1975 a, di Lonardo and Trombetti 1980, Carlotti *et al.* 1983) and $AsH_3$ (di Lonardo *et al.* 1984).

Another group of molecules which have been studied extensively are the methyl halides. Methyl fluoride, $CH_3F$, was one of the first molecules to be studied in detail at both Doppler-limited and sub-Doppler resolution (Freund *et al.* 1974). A series of measurements using both laser Stark and OODR methods (Brewer 1972, Shoemaker *et al.* 1974), which were tied to the accurately known MBER value of the ground-state dipole moment (Wofsy *et al.* 1971, Marshall and Muenter 1980), have allowed the variation of the dipole moment to be measured in some detail. It has also allowed the isotopic dependence of the dipole moment variation in the series $^{12}CH_3F$, $^{13}CH_3F$ and $^{12}CD_3F$ to be established (Duxbury *et al.* 1976, Duxbury and Freund 1977, Duxbury and Kato 1982). The results are summarized in table 4. It can be seen that the dipole moment change on excitation of the $v_3$ vibration of $CD_3F$ is approximately half that in the corresponding band in $CH_3F$. This has been explained by a vibrational mixing model (Duxbury *et al.* 1976). A small rotational dependence of the dipole moment has also been established. $CH_3F$ was the first optically pumped submillimetre laser to be demonstrated (Chang and Bridges 1970); it was also the first in which the assignments of the laser and pump transitions were unequivocally made. In some recent

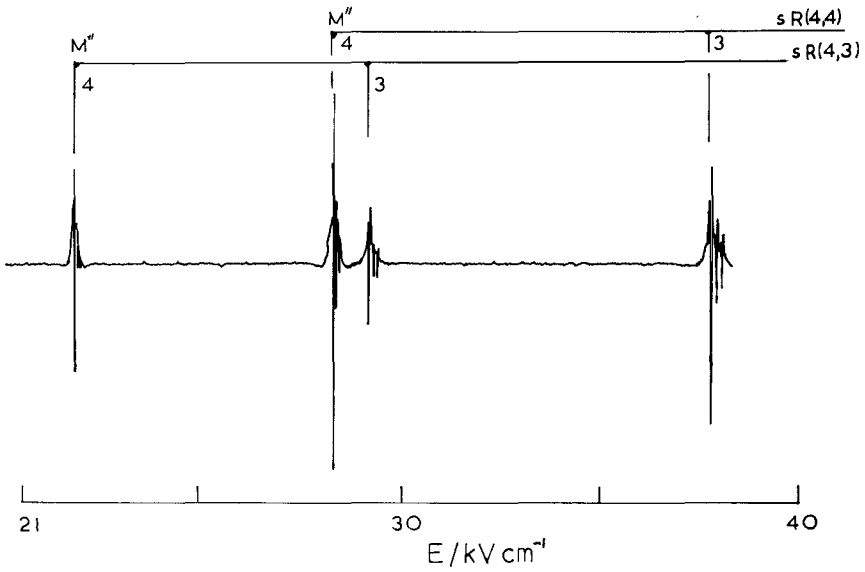


(*a*)

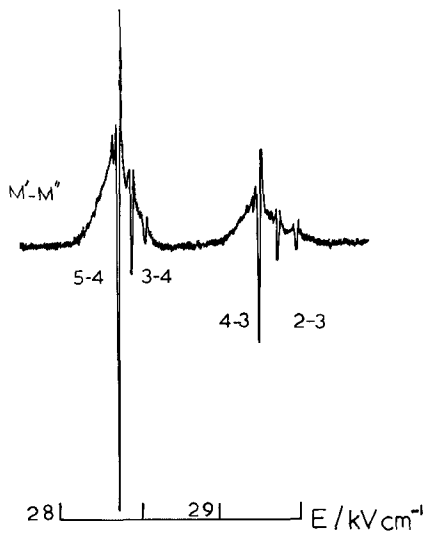


(*b*)

Figure 16. $^{s}R(4, K)$ transitions of $^{14}NH_3$ using the 9P(24) line of the $^{12}C^{18}O_2$ laser at 1065·756 $cm^{-1}$. The modulation amplitude was 3 V/cm and the time constant for detection 100 ms. (*a*) Broad scan showing the first members of the $^{s}R(4, 4)$ and the $^{s}R(4, 3)$ series. The main Stark shift is associated with the levels of the ground vibrational state. (*b*) Enlarged portion of the region of 28 to 30 kV/cm. The highest and lowest-frequency Lamb dips of each group are associated with transitions with $\Delta M_J = +1$ and $-1$ respectively, and the separation thus shows the size of the Stark shift in the excited state. The centre dip of each pattern is a velocity-tuned three-level resonance, whose intensity, $I_c$, is related to that of the two coupled transitions, $I_+$ and $I_-$ by

$$I_c = (I_+ I_-)^{1/2}$$

Table 4. Dipole moments (D) of $CH_3F$, $^{13}CH_3F$ and $CD_3F$.

| | $^{12}CH_3F$ | (Ref). | $^{13}CH_3F$ | Ref. | $^{12}CD_3F$ | Ref. |
|---|---|---|---|---|---|---|
| ground state | 1·8585(5) | (a) | 1·8579(6) | (b) | 1·8702(21) | (c) |
| $\nu_3$ | 1·9054(6) | (b) | 1·9039(6) | (b) | 1·8964(15) | (c) |
| $\nu_5$ | | | | | 1·8751(25) | (e) |
| $\nu_6$ | 1·859(5) | (f) | | | 1·8771(7) | (d) |
| $2\nu_3$ | 1·9519(20) | (b) | 1·951(4) | (b) | 1·9170(5) | (e) |
| $\nu_3+\nu_6$ | 1·909(5) | (f) | | | 1·932(7) | (f) |

(a) Marshall and Muenter (1980).
(b) Freund *et al.* (1974).
(c) Duxbury *et al.* (1976).
(d) Duxbury and Freund (1977).
(e) Caldow and Duxbury (1981).
(f) Duxbury and Kato (1982).

experiments OODR has been used to assign many other strong laser transitions in $CH_3F$ and its isotopomers, of which the most recent strong lasant investigated in this way has been $CHD_2F$ (McCombie and Duxbury 1985). In the OODR spectra of the $\nu_3$ and $\nu_5$ bands of $CD_3F$ strong evidence was found for very heavy mixing of some vibration–rotation levels (Duxbury and Kato 1982). This was confirmed by a rather full analysis of the four coupled bands $\nu_2$, $\nu_3$, $\nu_5$ and $\nu_6$ by Halonen *et al.* (1984). The significance of the existence of this strong mixing is that it may provide a rapid route for vibration–rotation relaxation to occur, and hence explain the much higher operation pressures which are possible in the $CD_3F$ laser compared to those which can be used with $CH_3F$ (Tobin *et al.* 1979, Chang and Bridges 1970). In addition to methyl fluoride, laser Stark spectra of $CH_3Cl$ (Shimizu 1975 b) $CD_3Cl$ (Yamada and Hirota 1977), $CD_3Br$ (Harada *et al.* 1983) and $CD_3I$ (Kawaguchi *et al.* 1977) have been analysed, and detailed study made of one of the silicon analogues, $SiH_3F$ (Escribano and Butcher 1983).

The molecule for which the most detailed dipole moment data is available is probably formaldehyde, $H_2CO$. The $\nu_2$ band was the first band of an asymmetric top molecule to be studied in detail (Johns and McKellar 1973). Since then the dipole moment has been measured in almost all the vibrational states of $H_2CO$, and in many of those in $D_2CO$ using CO and $CO_2$ laser Stark spectroscopy (table 5). The dipole moments in some of the excited vibrational levels involving the excitation of several quanta of $\nu_2$ and $\nu_4$ have been measured via the electronic spectrum using the stimulated emission PUMP and DUMP scheme in a Stark tuned system (Vaccaro *et al.* 1983). The dipole moment change associated with the excitation of $\nu_4$ is much larger than would normally be expected when an out-of-plane vibration is excited. This is thought to be associated with the large amplitude of the out-of-plane motion, so that the changes in the projections of the CO and CH bond moments from the bent configuration on to the planar molecule configuration are appreciable. The dipole moment variation in the other states is similar to that found in $CH_3F$, with the main change being associated with the excitation of the CO stretching mode, $\nu_2$. This latter change is almost identical in $D_2CO$, since in formaldehyde the CO stretching mode is almost an 'isolated' vibration, which contrasts with the behaviour seen in methyl fluoride.

### 6.2. *Dipole moments of non-polar molecules*

One of the most interesting types of dipole moment variation is seen in tetrahedral molecules such as methane. At the equilibrium geometry they possess no electric dipole

Table 5. Dipole moments (D) of formaldehyde, $H_2CO$, and thioformaldehyde, $H_2CS$, in various vibrational and electronic states.

| State | | $H_2CO$ | Ref | $H_2CS$ | Ref |
|---|---|---|---|---|---|
| $\tilde{X}, {}^1A_1$ | ground state | 2·3315(5) | (a) | 1·6491(4) | (a) |
| | $v_3=1$(CS), $v_2=1$(CO) | 2·3472(5) | (b, c) | 1·6576(12) | (b) |
| | $v_4=1$ | 2·3086(5) | (a) | 1·622(3) | (f) |
| | $v_6=1$ | 2·3285(5) | (a) | 1·642(5) | (f) |
| | $v_3=1$(CO) | 2·3250(25) | (e) | | |
| | $v_5=1$ | 2·2844(47) | (e) | | |
| | $v_2=2$ | 2·3605(20) | (e) | | |
| | $v_2=2$, $v_4=2$ | 2·3222(47) | (g) | | |
| | $v_2=1$, $v_4=4$ | 2·2825(33) | (g) | | |
| $\tilde{a}, {}^3A_2$ | | 1·29(3) | (h) | 0·534(15) | (j) |
| $\tilde{A}, {}^1A_2$ | | 1·56(7) | (i) | 0·838(8) | (j) |
| $\tilde{C}, {}^1B_1$ | | | | −2·20(20) | (k) |
| | | $D_2CO$ | | $D_2CS$ | |
| $\tilde{X}, {}^1A_1$ | ground state | 2·3471(5) | (e) | 1·6588(8) | (m) |
| | $v_3=1$(CS), $v_2=1$(CO) | 2·3672(15) | (e) | 1·661(3) | (f) |
| | $v_3=1$(CO) | 2·319(10) | (l) | | |
| | $v_6=1$ | 2·347(4) | (l) | | |

(a) Fabricant *et al.* (1977).
(b) Brechignac *et al.* (1982).
(c) Tanaka *et al.* (1982).
(d) Bedwell and Duxbury (1980).
(e) Allegrini *et al.* (1977).
(f) Duxbury *et al.* (1981).
(g) Vaccaro *et al.* (1983).
(h) Freeman and Klemperer (1966).
(i) Buckingham *et al.* (1970).
(j) Dixon and Gunson (1983).
(k) Goertz *et al.* (1981).
(l) Coffey *et al.* (1977).
(m) Cox *et al.* (1982).



moment, but under the influence of non-totally-symmetric vibrations the 'vibrationally averaged' dipole moment is non-zero. This can be considered to be the consequence of a vibrational Jahn–Teller effect. The original model of Mizushima and Venkateswarlu (1953) has been extended by Mills *et al.* (1969), and by Muenter and Dyke (1975).

A small dipole moment can also be induced if the symmetry is reduced from tetrahedral by isotopic substitution, for example by the replacement of one hydrogen atom by a deuterium atom to give $CH_3D$. This has been discussed in detail by Muenter and Dyke (1975).

The final method by which an electric dipole moment may be induced is by the effects of rotational distortion. This effect is most marked in molecules of tetrahedral symmetry, and the distortion needed to produce such an effect is shown in figure 17.

The principal experimental work in this area has been by Oka and his colleagues (Oka 1976). They have studied the induced dipole moments in the tetrahedral molecules $SiH_4$ (Kreiner *et al.* 1978) and $GeH_4$ (Kreiner *et al.* 1977) by a variety of methods including optical–optical double resonance and high-field Stark Lamb dip spectroscopy. In order to observe OODR spectra it is necessary to use very very small values of the modulator radio-frequency drive and very high values of the applied electric field. Typical spectra are shown in figures 18 and 19. The most recent OODR experiments on $CH_3D$ will be used to exemplify the main aspects of this work. $CH_3D$ has a small dipole moment of ca. $5{\cdot}6 \times 10^{-3}$ D which is due to the breakdown of

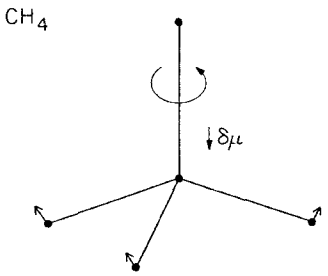


Figure 17. Centrifugal distortion-induced dipole moment in $CH_4$. (Reproduced by permission from *Molecular Spectroscopy: Modern Research*, Vol. 2, edited by K. N. Rao (Academic Press, 1976).)

tetrahedral symmetry. The $\theta$ parameters of $CH_3D$ can be related to those of $CH_4$ if the $\theta_\alpha^{\beta\gamma}$ are expressed in terms of the internal coordinates $S_m$ rather than the normal coordinates $Q_s$. Using this transformation Watson *et al.* (1979) showed that the parameters of $CH_3D$ could be predicted directly by using the single parameter $\theta_z^{xy}$ of methane (Ozier 1971) together with a knowledge of the well determined force field of methane.

### 6.3. *Polarizability changes in non-planar molecules*

A recent experiment on $CO_2$ has provided information on an important property, the vibrational dependence of the molecular polarizability tensor. An F-centre laser has been used to excite the $\nu_1 + \nu_3$ band of $CO_2$ at 3715 $cm^{-1}$ in a supersonic nozzle beam and the Stark spectrum was detected bolometrically (Gough *et al.* 1983). In order to measure the Stark splittings very high fields of up to 230 kV/cm were required. This allowed the splittings of the R(0) and the P(2) transitions to be measured very accurately. These data yielded the isotropic part, $(\alpha_n)$, and the anisotropic part, $(\Delta\alpha_n)$ of

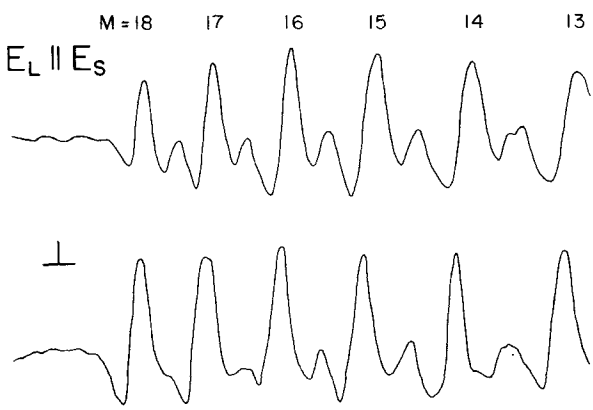


Figure 18. Part of the Stark Lamb dip spectrum of $SiH_4$ obtained using the $N_2O$ R(16) laser line. $E_L$ and $E_S$ refer to the direction of the laser polarization and the Stark field respectively. Trace (*a*) shows $\Delta M = 0$ and trace (*b*) $\Delta M = \pm 1$ transitions. The small lines between the main components are four-level collisionally transferred resonances. (Reproduced by permission from *Journal of Chemical Physics*, 1977, **68**, 3238.)

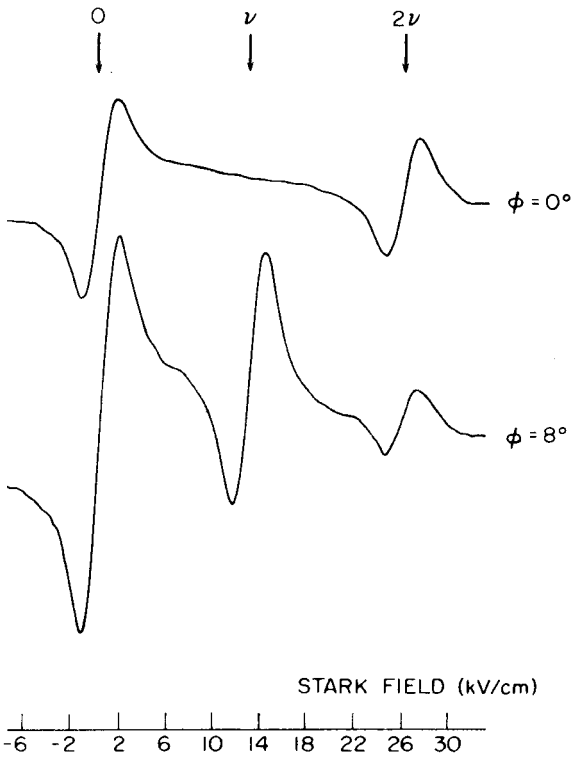


Figure 19. OODR spectra of $GeH_4$ observed using the $CO_2$ 10P(26) laser line. The radio-frequency driver of the EOM was set at $\nu = 1{\cdot}2290$ MHz. 0 denotes zero-field level crossing; $\nu$, signals due to $\nu_L$ and $\nu_L \pm \nu$; and $2\nu$, signals caused by the two sidebands $\nu_L \pm \nu$. The pressure of the gas was 5 mTorr and the time constant for detection 3 s. The two traces differ in the angular setting $\Phi$ of the wave plate of the electro-optic modulator. (Reproduced by permission from *Physics Review* A, 1977, **15**, 2300.)



the static polarizability in both the excited ($n=v$) and the ground ($n=0$) states. The direct observables were $\Delta\alpha_v/\Delta\alpha_0 = 1{\cdot}021(8)$, $(\alpha_v - \alpha_0)/\Delta\alpha_v = 0{\cdot}012(6)$ and $\Delta\alpha_v = 2{\cdot}65(18)$ Å$^3$. The result for $\Delta\alpha_v$ is 12% greater than that predicted for the static polarizability anisotropy, and the reason for this is not well understood. The other parameters are well predicted by the model proposed by Gough *et al.* (1983) to account for the vibrational dependence of $\alpha$.

### 6.4. *Effects of collisional energy transfer*

Much of the work on collisional energy transfer has stemmed from the pioneering work on Oka (1973). He pointed out that there are propensity rules, which resemble the selection rules for electric dipole transitions, for many of the collisional processes between dipolar molecules. In these soft collisions the molecule after a collision possesses a 'memory' of its state before the collision. In the early work there was little evidence for velocity selection effects since the majority of the experiments were carried out in the microwave region where the broadening processes are largely homogeneous (Oka 1973). However, in a set of infrared experiments using two-photon pumping and probing, Oka and his colleagues showed that in addition to the electric dipole

propensity rules, many dipolar collisions cause very little change in molecular velocity (Freund *et al.* 1973). Following these difficult experiments, it was realized that these effects could be seen 'routinely' in laser Stark Lamb dip and in OODR experiments as 'four-level resonances'.

Methyl fluoride was the first molecule in which four-level collisionally transferred resonances were clearly identified (Shoemaker *et al.* 1974, Johns *et al.* 1975 a). Subsequently these signals have been observed in many Stark spectra. Examples of strong four-level signals seen in $H_2CS$ and $CH_2NH$ are shown in figure 20. These demonstrate that in molecules in which the dipole moment is directed entirely along the principal near-symmetric rotor axis, a or c, the $\Delta M = \pm 1$ angular-momentum-tipping collisions are extremely selective. They also show that in molecules such as $CH_2NH$ (Duxbury *et al.* 1981) and $CH_3OH$ (Bedwell *et al.* 1978), where there is also a b



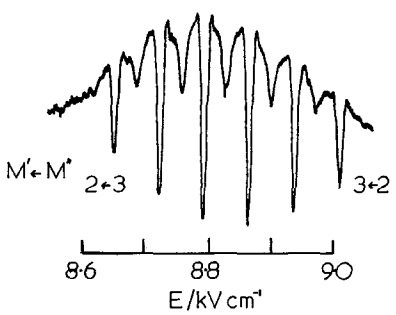


(*a*)

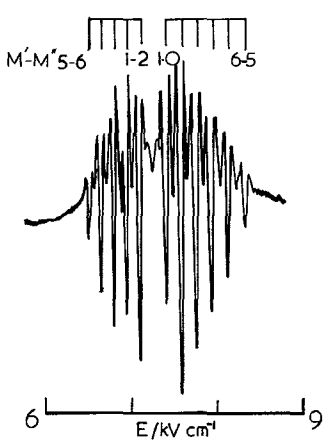


(*b*)

Figure 20. Lamb dip spectrum of the $^QQ$ branch transitions of $H_2CS$ and $CH_2NH$ using second-derivative presentation. (*a*) $^QQ(3,3)$ transitions of the $\nu_3$ band of $H_2CS$ observed using the 9P(32) line of a $^{12}C^{18}O_2$ laser. The gas pressure was 40 mTorr and the detection time constant 100 ms. (*b*) $^QQ(6,4)$ Coriolis-induced transition in the $\nu_9$ band of $CH_2NH$ observed using the 9R(12) line of a $CO_2$ laser. The gas pressure was 100 mTorr. Note the missing 0–1 transition. The resonances due to collisional energy transfer are proportionately much smaller in the asymmetric molecule.

component of the dipole moment, the four-level resonances are much less pronounced, indicating that collisional coupling to other rotational levels is now much more probable. Four-level resonances have also been observed in the $1_{11}-1_{01}$ transition of the $v_2$ band of $H_2^{17}O$, which possesses only a b component of the dipole moment (Johns and McKellar 1978). This set of energy levels constitute a very well isolated four-level system since the rotational constants of water are very large, and since it is a very asymmetric rotor. Although in the interpretation of the data there are some problems associated with power-broadening of the signals and with the presence of other isotopomers in the gas mixture, it was estimated that 3 to 15% of the collisions lead to a reorientation of $M_J$. The largest changes of $M_J$ recorded so far are in some transitions in $H_2CO$ where changes of $\Delta M_J$ or 4 or 6 have been found (Johns *et al.* 1975 b).

### 6.5. *Other molecular systems*

In addition to the examples described in this section spectra have been recorded for a variety of organic and inorganic molecules. References to the majority of the laser Stark and OODR experiments on stable molecules are given in table 6. Semi-stable molecules are considered separately in section 7.



## 7. Stark spectroscopy of semistable molecules

One of the principal advantages of laser spectrometers is their sensitivity for the detection of small quantities of short-lived species. The sensitivity of laser Stark spectrometers has been discussed by Freund *et al.* (1974) and by Johns and McKellar (1975). The latter group estimate that in an intracavity spectrometer with a pressure of 4 mTorr in a 20-cm long absorption cell, only about $10^6$ molecules are responsible for the Lamb dips seen on a particular vibration–rotation transition. This is close to Shimoda's estimate of the limiting sensitivity of a laser spectrometer (Shimoda 1973). This sensitivity has been exploited in studies of small 'semi-stable' molecules which, in Kroto's recent definition, have lifetimes of the order of seconds under the conditions of the gas-phase experiments (Kroto 1982).

The first short-lived molecule which was studied in detail (Johns and McKellar 1977 b) was HNO. They used a Stark cell located inside the cavity of a CO laser. The HNO molecules were produced in a transverse flow system by the reaction $H+NO\rightarrow HNO$. In order to keep the pressure in the Stark cell low, a pinhole separated the high-pressure region of atom production from the low-pressure reaction region close to the plates. In this system, high-quality Lamb dip spectra were obtained as shown in figure 21. From these spectra accurate values of the band origins and rotational constants of the $v_2$ (N–O stretching) bands of HNO and DNO were obtained, and also of the $v_3$ (bending) vibrational band of HNO. A few transitions in the $v_1$ (N–D stretching) band of DNO were also detected. This study confirmed the value of $1500\,cm^{-1}$ for the $v_3$ frequency of HNO which has been obtained from the analysis of the electronic spectrum (Clough *et al.* 1973), and from the most recent matrix isolation studies (Jacox and Milligan 1973). Previous values of this frequency, obtained from earlier matrix isolation experiments, had been ca. $1100\,cm^{-1}$. Since the $v_2$ and $v_3$ vibrational states of HNO are separated by only $65\,cm^{-1}$ it was necessary to include the c-axis Coriolis coupling between these two states. In the determination of the dipole moments it proved to be possible to obtain both the a and the b components, $\mu_a$ and $\mu_b$, in the ground state, owing to the occurrence of some accidental coincidences. However, in the excited state only $\mu_a$ could be determined. Recently the infrared spectrum of

Table 6. Stable molecules studied by laser Stark spectroscopy.

| Molecule | Laser | Vibrational bands | Method | Reference |
|---|---|---|---|---|
| $D^{79}Br$ | CO | 1–0 | LS–LD, FT | Herman *et al.* (1982) |
| NO | CO | 1–0 | LS–LD, LC | Hoy *et al.* (1975) |
| DCN | CO | 001–000, $01^10$–$01^10$ | LS | Maki and Freund (1982) |
| $DC^{15}N$ | CO | 001–000 | | |
| $CO_2$ | F-centre | $\nu_1+\nu_3$ | TS–bol | Gough *et al.* (1983) |
| OCS | $CO_2$ | $02^00$–$00^00$, $03^10$–$01^10$ | LS | Maki and Freund (1976) |
| OCS | $CO_2$ | $03^10$–$01^10$, $04^00$–$02^00$ | LS | Nakagawa *et al.* (1976) |
| OCS | $CO_2$ | $03^10$–$01^10$ | Ls–m | Tanaka and Tanaka (1978) |
| OCS | $CO_2$ | $02^00$–$00^00$, 200–000 $12^00$–$00^00$ | Ls–m LS–LD | Tanaka *et al.* (1984) |
| FCN | $CO_2$ | $\nu_3$ and hot bands | LS | Maki and Freund (1977) |
| $D_2O$ | HCN | pure rotation | LS | Duxbury and Jones (1971 a) Brittain *et al.* (1972) |
| $H_2{}^{17}O$ $H_2{}^{18}O$ | CO | 010–000 | LS–LD | Johns and McKellar (1978) |
| $H_2{}^{16}O$ | CO | 020–010 | LS–LD, IR–RF–DR | Herman *et al.* (1979) |
| FNO | CO | 100–000 | LS–LD | Allegrini *et al.* (1978) |
| $ClO_2$ | $CO_2$, $N_2O$ | $\nu_1$ | LS | Tanaka and Tanaka (1983) |
| HCCF | $CO_2$ | $\nu_3$, $\nu_3+\nu_4-\nu_4$, $\nu_3+\nu_5-\nu_5$ | LS | Tanaka *et al.* (1976) |
| DCCF | $CO_2$ | $\nu_3$ and hot bands | LS–m | Matsumura *et al.* (1980) |
| $^{14}NH_3$ | $D_2O$, pulsed | rotation–inversion | LS | Shimizu *et al.* (1968) |
| $^{14}NH_3$ | $CO_2$, $N_2O$ | $\nu_3$ | LS | Shimizu (1969, 1970 a) |
| $^{14}NH_2D$ | $CO_2$ | $\nu_2$ | LS–LD | Brewer *et al.* (1969) |
| $^{15}NH_3$ | $CO_2$, $N_2O$ | $\nu_2$ | LS | Shimizu (1970 b) |
| $^{14}ND_3$ | DCN | rotation–inversion | LS | Duxbury and Jones (1971 b) |
| $^{14}NH_3$ | $CO_2$, $N_2O$ | $\nu_2$ | LS | Ueda and Shimoda (1975) |
| $^{14}NH_3$ | CO | $2\nu_2$ and $\nu_4$ | LS–LD | Johns *et al.* (1975 b) |
| $^{14}NH_3$ | $CO_2$ | $2\nu_2$ | 2p | Bischel *et al.* (1976) |
| $^{14}NH_3$ | $CO_2$ | $\nu_2$, $\Delta k=\pm 3$ | LS | Laughton *et al.* (1976) |
| $^{15}NH_3$ | $CO_2$ | $\nu_2$ | OODR | Orr and Oka (1977 b) |
| $^{14}NH_3$ | $CO_2$ | $2\nu_2-\nu_2$ | LS–LD | Takami *et al.* (1979) |
| $^{14}NH_2D$ | $CO_2$ | $\nu_2$ | LS–s–LD | Rackley and Butcher (1980) |
| $^{14}NH_3$ $^{15}NH_3$ $^{14}NH_2D$ | $CO_2$ | | LS | Shimoda *et al.* (1980 a, b) |
| $^{15}NH_3$ | $CO_2$ | $\nu_2$ | LS–LD | di Lonardo *et al.* (1981) |
| $^{14}ND_3$ | $CO_2$ | $\nu_2$ | LS–LD | di Lonardo and Trombetti (1981) |
| $^{14}NH_3$ | CO | $2\nu_2$ and $\nu_4$ | LS | Sasada *et al.* (1982) |
| $^{14}NH_3$ | $CO_2$ | $\nu_2$ | Ls–oad LD | di Lieto *et al.* (1982) |
| $^{14}NH_3$ | $CO_2$ | $\nu_2$ | LS–oad LD | Minguzzi *et al.* (1982) |
| $^{14}NH_3$ | CO | $2\nu_2$ and $\nu_4$ | LS–LD | Weber and Terhune (1982) |
| $^{15}NH_3$ | $CO_2$ | $\nu_2$ | OODR | Duxbury *et al.* (1984) |
| $PH_3$ | $CO_2$ | $\nu_2$ | LS–s | Shimizu (1972) |
| $PH_3$ | $CO_2$, $N_2O$ | $\nu_2$, $\nu_4$ | LS | Shimizu (1975 a) |
| $PH_3$ | $CO_2$ | $\nu_2$ | OODR | Orr and Oka (1980) |
| $PH_3$ | $CO_2$ | $\nu_2$, $\nu_4$ | LS–LD | di Lonardo and Trombetti (1980) |
| $PH_3$ | $CO_2$ | $\nu_2$, k = 3 doubling | LS–LD | Carlotti *et al.* (1983) |
| $PH_3$ | $CO_2$ | $2\nu_2$ | LS–2p | Takagi (1984) |
| $AsH_3$ | $CO_2$ | $\nu_2$ | LS–LD | di Lonardo *et al.* (1984) |
| $H_2CO$ $D_2CO$ | CO | $\nu_2$ | LS | Johns and McKellar (1973) |
| $H_2CO$ | CO | $2\nu_2-\nu_2$ | LS–LD | Johns and McKellar (1975) |

Table 6 (*continued*)

| | | | | |
|---|---|---|---|---|
| $D_2CO$ | $CO_2$ | $\nu_4, \nu_6$ | LS | Coffey *et al.* (1977) |
| HDCO | CO | $\nu_3$ | LS–LD | Johns and McKellar (1977 a) |
| $H_2CO$ | CO | $\nu_3$ | LS–LD | Allegrini *et al.* (1977 a) |
| $H_2CO$ | CO | $\nu_5-\nu_6$ | LS, GR | Allegrini *et al.* (1977 b) |
| $H_2CO$ | CO | $\nu_2$ | Ls–m | K. Tanaka *et al.* (1982) |
| $H_2CO$ | CO | $\nu_2$ | LS–LD, FT | Brechignac *et al.* (1982) |
| HFCO | CO | $\nu_2$ | LS–LD, FT | Wong *et al.* (1982) |
| $CH_3D$ | $CO_2$ | $\nu_6$ | OODR | Watson *et al.* (1979) |
| $SiH_4$ | $CO_2$ | $\nu_2$ | LS–LD | Kreiner *et al.* (1978) |
| $GeH_4$ | $CO_2$ | $\nu_2$ | OODR | Kreiner *et al.* (1977) |
| $CH_3F$ | $CO_2$ | $\nu_3$ | OODR | Brewer (1970) |
| $CH_3F$ | HeNe | $\nu_1$ | LS–LD | Luntz *et al.* (1969) |
| $^{12}CH_3F$ $^{13}CH_3F$ | $CO_2$ | $\nu_3, 2\nu_3-\nu_3$ | LS | Herlemont *et al.* (1973) |
| $^{12}CH_3F$ $^{13}CH_3F$ | $CO_2$ | $\nu_3, 2\nu_3-\nu_3$ | LS–LD | Freund *et al.* (1974) |
| $^{12}CH_3F$ $^{13}CH_3F$ | $CO_2$ | $\nu_3$ | OODR | Shoemaker *et al.* (1974) |
| $CH_3F$ | $CO_2$ | $2\nu_3$ | LS–2p | Bischel *et al.* (1975) |
| $CH_3F$ | $CO_2$ | $\nu_3$ | OODR | Orr and Oka (1977 a) |
| $CD_3F$ | $CO_2$ | $\nu_3$ | LS–LD | Duxbury *et al.* (1976) |
| $CD_3F$ | $CO_2$ | $\nu_6$ | LS–LD | Duxbury and Freund (1977) |
| $CD_3F$ | $CO_2$ | $\nu_5$ | LS–LD | Caldow and Duxbury (1981) |
| $CH_3F$ | $CO_2$ | $2\nu_3-\nu_3$ | LS–beam | Matsushima *et al.* (1981) |
| $^{12}CH_3F$ | $CO_2$ | $\nu_3, 2\nu_3-\nu_3$ $\nu_3+\nu_6-\nu_6$ | OODR | Duxbury and Kato (1982) |
| $^{13}CH_3F$ | | $\nu_3, 2\nu_3-\nu_3$ | | |
| $CD_3F$ | | $\nu_3, \nu_5, \nu_6, \nu_3+\nu_6-\nu_6$ | | |
| $CH_3F$ | $CO_2$ | $\nu_3$ | LS–bol | Douketis and Gough (1983) |
| $^{13}CH_3F$ | $CO_2$ | $\nu_3$ | LC | Sandholm and Schwendeman (1983) |
| $CH_3{}^{35}Cl$ | $CO_2$ | $\nu_6$ | LS | Shimizu (1975 b) |
| $CD_3{}^{35}Cl$ | $CO_2$ | $\nu_2, \nu_5$ | LS | Yamada and Hirota (1977) |
| $CH_3{}^{35}Cl$ $CH_3{}^{37}Cl$ | $CO_2$ | $\nu_6$ | LS–LD | Golby and Butcher (1984) |
| $CH_3Br$ | $CO_2$, $N_2O$ | $\nu_6$ | LS | Ieki *et al.* (1978) |
| $CD_3Br$ | $CO_2$ | $\nu_2, \nu_5$ | LS | Harada *et al.* (1983) |
| $CD_3I$ | $CO_2$ | $\nu_2$ | LC | Sakai and Katayama (1975) |
| $CD_3I$ | $CO_2$ | $\nu_2$ | AC | Sakai and Katayama (1976) |
| $CD_3I$ | $CO_2$, $N_2O$ | $\nu_2$ | LS | Kawaguchi *et al.* (1977) |
| $CD_3I$ | $CO_2$ | $\nu_2$ | LC<br>LS–LD | Caldow *et al.* (1978) |
| $CDF_3$ | $CO_2$ | $\nu_5$ | LS | Ibisch and Andresen (1980) |
| $CDF_3$ | $CO_2$ | $\nu_5$ | LS–m<br>LS–LD | Harada *et al.* (1984) |
| $SiH_3F$ | $CO_2$ | $\nu_2, \nu_5$ | LS–LD | Escribano and Butcher (1983) |
| $CH_2F_2$ | $CO_2$ | $\nu_9$ | LS | Kawaguchi and Tanaka (1977) |
| $POF_3$ | $CO_2$ | $\nu_4$ | LS | Amano and Schwendeman (1978) |
| $POF_3$ | $CO_2$ | $\nu_4$ | AC | Amano and Schwendeman (1979) |
| HCOOH | CO | $\nu_3$ | LS, diode | Kuze *et al.* (1982) |
| $CH_2CF_2$ | $CO_2$, $N_2O$ | $\nu_4, \nu_9$ | LS | Duxbury *et al.* (1974) |
| $CH_2CF_2$ | $CO_2$, $N_2O$ | $\nu_4, \nu_9$ | LS–LD | Duxbury and Herman (1978) |
| $CH_3OH$ | $CO_2$ | CO stretch fundamental | LS–LD<br>OODR | Bedwell *et al.* (1978) |
| $CH_3OH$ | $CH_3OH$ | Stark effect on opt. pumped laser trans. | LS | Henningsen (1980) |
| $CH_3OH$ | $CO_2$ | CO stretch fundamental | OODR | Bedwell and Duxbury (1979) |

Table 6 (*continued*)

| Molecule | Laser | Vibrational bands | Method | Reference |
|---|---|---|---|---|
| $CH_3OH$ | HCN | torsion–rotation | LS | Johnston *et al.* (1980) |
| $CH_3OH$ | $CH_3OH$ | Stark effect on opt. pumped laser trans. | LS–LD | Henningsen (1982) |
| $CH_3OH$ | $CO_2$ | CO stretch fundamental | LS–m | Amano (1981) |
| $CH_3OH$ | $CO_2$ | CO stretch fundamental $CH_3$ in plane rock | OODR | Duxbury *et al.* (1984) |
| $CH_3CN$ | $CO_2$ | $\nu_4, \nu_7, 3\nu_8$ | LS | Rackley *et al.* (1982) |
| $CH_3CN$ | $CO_2$ | $\nu_4$ | LC | Sandholm *et al.* (1983) |
| $C^{15}H_3CN$ | $CO_2$ | $\nu_4$ | LS | Mito *et al.* (1984 a) |
| $C^{15}H_3CN$ | $CO_2$ | $\nu_4+\nu_8-\nu_8$ | LS | Mito *et al.* (1984 b) |
| $CH_3CCH$ | $CO_2$ | $\nu_5$ | LS | Burrell *et al.* (1980) |
| $CH_3CCH$ | $CO_2$ | $\nu_5$ | LS, SISAM | Meyer *et al.* (1982) |

Key to methods

| | |
|---|---|
| LS | Laser Stark spectroscopy. |
| LS–LD | LS with Lamb dip (sub-Doppler) resolution. |
| LS–s | LS with RF sidebands. |
| LS–m | LS with high field microwave double resonance. |
| LS–beam | LS with a molecular beam spectrometer. |
| LS–bol | LS–beam with bolometric detection. |
| LS–oad | LS with optoacoustic detection. |
| LS–2p | two-photon spectroscopy with laser Stark tuning. |
| TS | tuned laser spectroscopy with very high Stark field. |
| FT | LS combined with data from Fourier transform spectrometer. |
| GR | LS combined with data from grating infrared spectrometer. |
| SISAM | LS combined with data from SISAM spectrometer. |
| diode | LS combined with data from diode laser spectrometer. |
| IR–RF–DR | LS combined with data from infrared radio-frequency double resonance. |



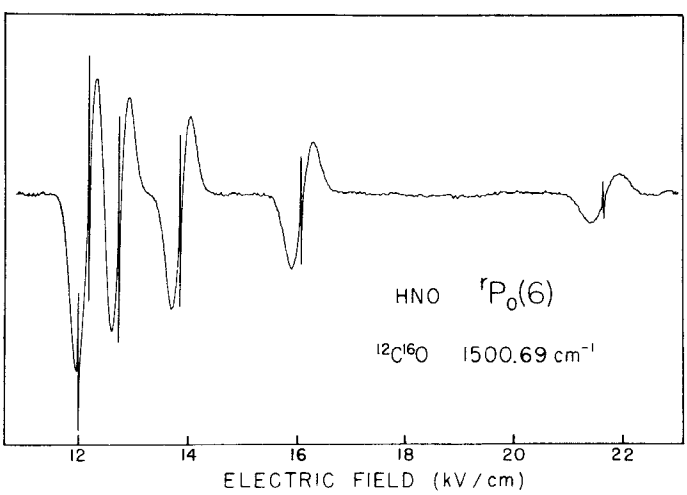


Figure 21. Intractivity laser Stark spectrum of the $\nu_3$ band of HNO recorded with the 24–23 (P(16) line of a CO laser and parallel polarization. This series is one of a number observed which involve the 'accidental' coincidence of the $5_{15}$ and $6_{06}$ levels in the ground state, and which are due to the *b* component of the dipole moment. Sharp Lamb dips can be seen on all the Doppler-broadened resonances. (Reproduced by permission from *Journal of Chemical Physics*, 1977, **66**, 1220.)

HNO has been reinvestigated by Johns *et al.* (1983) using a high-resolution Fourier-transform spectrometer. Despite the advantage of the wide frequency coverage of the FTS, the lack of sensitivity relative to the previous laser method was demonstrated by the inability to observe the $\nu_3$ band which they had previously recorded by the laser Stark method.

Another semi-stable molecule which has been studied in considerable detail is thioformaldehyde, $H_2CS$. Until quite recently thioformaldehyde was known only as a trimer, the first evidence for the existence of the monomer being in mass spectrometric studies. Interest in the species developed following the observation of the microwave spectrum of HCS by Johnson and Powell (1970), and its subsequent detection in the interstellar dust clouds by microwave radioastronomy (Sinclair *et al.* 1973). The first high-resolution infrared spectrum of the 3 $\mu$m bands was obtained by Johns and Olson (1971). This required both a very long path length and a high gas pressure, and was a *tour de force* with a diffraction grating instrument.

Laser techniques were first employed in the infrared region when the 10 $\mu$m band system was observed using a laser Stark spectrometer with a multiple-pass Stark cell (Bedwell and Duxbury 1977, 1980). The thioformaldehyde was produced by the pyrolysis of dimethyl disulphide. The pyrolysis products, which include $CH_3$ and $CH_3SH$, flowed continuously through the cell. With short time-constants of 100 to 300 ms a very high signal-to-noise ratio was obtained (figure 20), even though the total gas pressure in the cell was only 10 mTorr.

In the 10 $\mu$m region three fundamental vibration–rotation bands were observed, $\nu_3$, $\nu_4$ and $\nu_6$, rather than the two, $\nu_3$ and $\nu_4$, expected on the basis of the analysis of the matrix isolation spectra (Jacox and Milligan 1975 b). Two of the bands, $\nu_4$ and $\nu_6$, are separated by only 1 $cm^{-1}$ and hence were unresolved in the matrix studies. Since these states are almost degenerate and there is strong Coriolis coupling between them, their energy level pattern closely resembles that of a degenerate vibrational state of a symmetric rotor molecule. Until this strong interaction was recognized, the complex Stark patterns observed on almost all the 9 and 10 $\mu$m lines of the $CO_2$ laser provided an intriguing puzzle. Owing to the high resolution and sensitivity of the Lamb dip method in a crossover multiple-pass cell, the vibrational change in dipole moment could be measured very accurately, and many strong signals due to collisional energy transfer were observed. These results have been combined with OODR (Duxbury *et al.* 1981) and molecular-beam electric resonance results (Fabricant *et al.* 1977) to give a very detailed picture of the vibrational dependence of the dipole moment. These results are compared, in table 5, with similar data obtained for $H_2CO$.

A second semistable molecule produced by pyrolysis is methyleneimine, $CH_2NH$. This is produced by the pyrolysis of primary amines, particularly methylamine. The first band to be analysed in detail was the $\nu_4$ band by Allegrini *et al.* (1979), using the NRCC intracavity CO laser spectrometer. The 10 $\mu$m bands were being studied at about the same time by Duxbury and his colleagues, but the analysis was fragmentary as the spectra presented an apparently random set of patterns. This complex structure proved to be due to the very strong Coriolis interaction between the three close-lying bands $\nu_7$, $\nu_8$ and $\nu_9$ (Jacox and Milligan 1975 a). A preliminary analysis of some of the Stark patterns was given by Duxbury *et al.* (1981), and by Duxbury and LeLerre (1984). However, the detailed analysis of these bands has become possible only through a combination of laser Stark and Fourier transform spectra (Halonen and Duxbury 1985, Duxbury *et al.* 1985). Methyleneimine, like thioformaldehyde, is one of the molecules found by radioastronomy in the interstellar dust clouds. These laser data should facilitate the detection of these species by infrared astronomy.

The only short-lived free radical tackled by laser Stark methods had been HCO, which was studied by Landsberg *et al.* (1977). In a very difficult experiment they succeeded in observing the $CO_2$ laser electric resonance spectrum of the $v_2$ band of HCO produced by the reaction of $H_2CO$ with fluorine atoms. Since this band has also been studied by 10 $\mu$m L.M.R. (Johns *et al.* 1977), these parallel studies have provided a good opportunity to compare the relative merits of the laser Stark and laser magnetic resonance methods. In their paper, Landsberg and his colleagues summarized the disadvantages of laser Stark spectroscopy for free radical studies as:

(1) Much lower gas pressures of the reagents are needed than in L.M.R. so that electric breakdown can be avoided.
(2) Signals are obtained from all the molecules with an electric dipole moment which are present in the discharge, since the paramagnetic species are not modulated preferentially (although Zeeman double modulation could be used).
(3) The Stark tuning is small for rotational levels with large values of $N$.
(4) The energy matrix which needs to be diagonalized is large because of parity mixing.

The advantages of laser Stark spectroscopy may be summarized as:

(*a*) The method is not restricted to free radicals, and polar molecules (e.g. HNO) can be studied.
(*b*) At any value of the applied field the transitions are allowed through the electric dipole moment, whereas in L.M.R. the transition moment may be lost for resonances with large shifts.
(*c*) The apparatus is simpler to build and the light-path is longer.

A summary of the experimental results on HNO, $H_2CS$, $CH_2NH$ and HCO, together with those on other species which might be considered to be 'semi-stable' is given in table 7.



Table 7. Laser Stark spectra of some semistable molecules.

| Molecule | Laser | Vibrational band | Method† | Reference |
|---|---|---|---|---|
| HNO | CO | $v_2, v_3$ | LS–LD | Johns and McKellar (1977 b) |
| DNO | CO | $v_1$ | LS–LD | Johns and McKellar (1977 b) |
| HCO | CO | $v_1$ | LS | Landsberg *et al.* (1977) |
| $CH_2NH$ | CO | $v_4$ | LS–LD | Allegrini *et al.* (1979) |
| $CH_2NH$ | $CO_2$ | $v_7, v_9$ | LS–LD | Duxbury *et al.* (1981, 1985) |
| $CH_2NH$ | $CO_2$ | $v_8$ | LS–LD | Duxbury and Le Lerre (1984) |
| $H_2CS$ | $CO_2$ | $v_3, v_5, v_6$ | LS–LD | Bedwell and Duxbury (1980) |
| | | | OODR | Duxbury *et al.* (1981) |
| $D_2CS$ | $CO_2$ | $v_3$ | LS–LD | Duxbury *et al.* (1981) |
| $HNO_2$ | CO | $v_2$ cis | LS–LD | Allegrini *et al.* (1980) |
| $CH_2NOH$ | $CO_2$ | $v_8$ | OODR | Duxbury *et al.* (1982) |

† Methods as in table 6.

## 8. Conclusion

The previous sections describe some of the progress that has been made in the application of the Stark effect in laser spectroscopy since the first experiments in 1966. These methods have allowed us to gain an insight into the vibrational and rotational dependence of the dipole moment, particularly of 'non-polar' molecules. They have

also provided high-quality spectroscopic data for a variety of small molecules. The sensitivity of these types of laser spectrometers is sufficiently high that they have enabled the study of several important semi-stable molecules to be carried out. Finally, they have provided an important route to studying the energy transfer processes in small molecules, not only by the observation of collisionally transferred saturation features, but also by permitting the detailed study of many of the pump transitions of the optically pumped submillimetre gas lasers.

## Acknowledgments

The author is particularly grateful to his colleagues and former colleagues, R. G. Jones, S. M. Freund, T. Oka, A. R. W. McKellar, J. W. C. Johns, H. Herman, D. J. Bedwell, G. L. Caldow, M. L. Le Lerre, C. A. Orengo, L. A. Evans, C. A. Williams, M. Taylor, J. C. Petersen, J. McCombie, H. Kato, D. Devoy, R. Boodaghians and M. Percival for their contribution to many of the topics mentioned in this review.

## References

ALLEGRINI, M., JOHNS, J. W. C., and MCKELLAR, A. R. W., 1977, *J. molec. Spectrosc.*, **67,** 476.
ALLEGRINI, M., JOHNS, J. W. C., and MCKELLAR, A. R. W., 1978, *J. molec. Spectrosc.*, **73,** 168.
ALLEGRINI, M., JOHNS, J. W. C., and MCKELLAR, A. R. W., 1979, *J. molec. Spectrosc.*, **70,** 2829.
ALLEGRINI, M. JOHNS, J. W. C., MCKELLAR, A. R. W., and PINSON, P., 1980, *J. molec. Spectrosc.*, **79,** 446.
AMANO, T., and SCHWENDEMAN, R. H., 1978, *J. chem. Phys.*, **68,** 530.
AMANO, T., and SCHWENDEMAN, R. H., 1979, *J. molec. Spectrosc.*, **78,** 437.
AMANO, T., 1981, *J. molec. Spectrosc.*, **88,** 194.
AUTLER, S. H., and TOWNES, C. H., 1955, *Phys. Rev.*, **100,** 703.
BEDWELL, D. J., and DUXBURY, G., 1977, *XXI Colloque International d'Astrophysique*, p. 434.
BEDWELL, D. J., DUXBURY, G., HERMAN, H., and ORENGO, C. A., 1978, *Infrared Phys.*, **18,** 453.
BEDWELL, D. J., and DUXBURY, G., 1979, *Chem. Phys.*, **37,** 445.
BEDWELL, D. J., and DUXBURY, G., 1980, *J. molec. Spectrosc.*, **84,** 53.
BISCHEL, W. K., KELLY, P. J., and RHODES, C. K., 1975, *Phys. Rev. Lett.*, **34,** 300.
BISCHEL, W. K., KELLY, P. J., and RHODES, C. K., 1976, *Phys. Rev.* A, **13,** 1829.
BOGAARD, M. P., and ORR, B. J., 1975, *International Review of Science, Physical Chemistry.* Series Two, Vol. 2, edited by A. D. Buckingham (London: Butterworth), p. 149.
BRECHIGNAC, C., JOHNS, J. W. C., MCKELLAR, A. R. W., and WONG, M., 1982, *J. molec. Spectrosc.*, **96,** 353.
BREWER, R. G., KELLY, M. J., and JAVAN, A., 1969, *Phys. Rev. Lett.*, **23,** 559.
BREWER, R. G., 1970, *Phys. Rev. Lett.*, **25,** 1639.
BREWER, R. G., and SWALEN, J. D., 1970, *J. chem. Phys.*, **52,** 2774.
BREWER, R. G., 1972, *Science*, **178,** 247.
BREWER, R. G., SHOEMAKER, R. L., and STENHOLM, S., 1974, *Phys. Rev. Lett.*, **33,** 63.
BRIDGE, N. J., HANER, D. A., and DOWS, D. A., 1968, *J. chem. Phys.*, **48,** 4916.
BRITTAIN, A., COX, A. P., DUXBURY, G., HERSEY, T. G., and JONES, R. G., 1972, *Molec. Phys.*, **24,** 843.
BUCKINGHAM, A. D., 1972, *International Review of Science*, Physical Chemistry Series 1, Vol. 3, edited by D. A. Ramsay (London: Butterworth), p. 73.
BUCKINGHAM, A. D., and RAMSAY, D. A., 1965, *J. chem. Phys.*, **42,** 3721.
BUCKINGHAM, A. D., and RAMSAY, D. A., 1965,
BUCKINGHAM, A. D., RAMSAY, D. A., and TYRRELL, J., 1970, *Canad. J. Phys.*, **48,** 1242.
BURRELL, P. M., BJARNHOF, E., and SCHWENDEMAN, R. H., 1980, *J. molec. Spectrosc.*, **69,** 239.
CALDOW, G. L., DUXBURY, G., and EVANS, L. A., 1978, *J. molec. Spectrosc.*, **69,** 239.
CALDOW, G. L., and DUXBURY, G., 1981, *J. molec. Spectrosc.*, **89,** 93.
CARLOTTI, M., DI LONARDO, G., and TROMBETTI, A., 1983, *J. chem. Phys.*, **78,** 1670.
CHANG, T. Y., and BRIDGES, T. J., 1970, *Opt. Commun.*, **1,** 423.
CLOUGH, P. N., THRUSH, B. A., RAMSAY, D. A., and STAMPER, J. G., 1973, *Chem. Phys. Lett.*, **23,** 155.

COFFEY, D., YAMADA, A., and HIROTA, E., 1977, *J. molec. Spectrosc.*, **64,** 98.
COX, A. P., HUBBARD, S. D., and KATO, H., 1982, *J. molec. Spectrosc.*, **93,** 196.
DALE, R. M., HERMAN, M., JOHNS, J. W. C., MCKELLAR, A. R. W., NAGLER, S., and STRATHY, I. K. M., 1979, *Canad. J. Phys.*, **57,** 677.
DI LONARDO, G., and TROMBETTI, A., 1980, *Chem. Phys. Lett.*, **76,** 307.
DI LONARDO, G., TROMBETTI, A., and VELINO, B., 1981, *Chem. Phys. Lett.*, **80,** 352.
DI LONARDO, G., and TROMBETTI, A., 1981, *Chem. Phys. Lett.*, **84,** 327.
DI LONARDO, G., FUSINA, L., and TROMBETTI, A., 1984, *Chem. Phys. Lett.*, **110,** 513.
DI LIETO, A., MINGUZZI, P., and TONELLI, M., 1982, *Appl. Phys.* B, **27,** 1.
DIXON, R. N., and GUNSON, M. R., 1983, *J. molec. Spectrosc.*, **101,** 369.
DOUKETIS, C., and GOUGH, T. E., 1983, *J. molec. Spectrosc.*, **101,** 325.
DUXBURY, G., and JONES, R. G., 1971 a, *Molec. Phys.*, **20,** 721.
DUXBURY, G., and JONES, R. G., 1971 b, *Chem. Phys. Lett.*, **8,** 439.
DUXBURY, G., FREUND, S. M., and JOHNS, J. W. C., 1976, *J. molec. Spectrosc.*, **62,** 99.
DUXBURY, G., and FREUND, S. M., 1977, *J. molec. Spectrosc.*, **67,** 219.
DUXBURY, G., GAMBLE, T. J., and HERMAN, H., 1974, *IEEE Trans. microw. Theory Tech.*, **MTT-22,** 1108.
DUXBURY, G., and HERMAN, H., 1978, *J. molec. Spectrosc.*, **73,** 444.
DUXBURY, G., KATO, H., and LE LERRE, M. L., 1981, *Faraday Discuss. Chem. Soc.*, **71,** 97.
DUXBURY, G., and KATO, H., 1982, *Chem. Phys.*, **66,** 161.
DUXBURY, G., KATO, H., and ROBINSON, D., 1982, *J. molec. Struct.*, **80,** 371.
DUXBURY, G., 1983, *Chem. Soc. Rev.*, **12,** 453.
DUXBURY, G., KATO, H., LE LERRE, M. L., MCCOMBIE, J., and PETERSEN, J. C., 1983, *Quantum Electronics and Electron Optics*, edited by P. L. Knight (New York: Wiley), p. 191.
DUXBURY, G., PETERSEN, J. C., KATO, H., and LE LERRE, M. L., 1984, *J. molec. Spectrosc.*, **107,** 261.
DUXBURY, G., and LE LERRE, M. L., 1984, *Infrared Phys.*, **24,** 261.
DUXBURY, G., LE LERRE, M. L., and LEMOINE, B., 1985 (to be published).
ESCRIBANO, R., and BUTCHER, R. J., 1983, *J. molec. Spectrosc.*, **99,** 450.
EVENSON, K. M., SAYKALLY, R. J., JENNINGS, D. A., CURL, R. F., and BROWN, J. M., 1980, *Chemical and Biochemical Applications of Lasers*, edited by C. B. Moore, Vol. 5, (New York: Academic Press), p. 95.
FABRICANT, B., KREIGER, D., and MUENTER, J. S., 1977, *J. Chem. Phys.*, **67,** 1576.
FELD, M. S., SANCHEZ, A., JAVAN, A., and FELDMAN, B. J., 1974, *Methodes de Spectroscopie sans Largeur Doppler des Niveaux Excites de Systemes Moleculaires Simples*, CNRS No. 217, 87.
FREED, C., and JAVAN, A., 1970, *Appl. Phys. Lett.*, **17,** 53.
FREED, C., BRADLEY, L. C., and O'DONNELL, G. R., 1980, *IEEE Jl quant. Electron.*, **QE-16,** 1195.
FREEMAN, D. E., and KLEMPERER, W., 1966, *J. chem. Phys.*, **45,** 52.
FREUND, S. M., JOHNS, J. W. C., MCKELLAR, A. R. W., and OKA, T., 1973, *J. chem. Phys.*, **59,** 3445.
FREUND, S. M., DUXBURY, G., ROMHELD, M., TIEDJE, J. T., and OKA, T., 1974, *J. molec. Spectrosc.*, **52,** 38.
GOERTZ, W., MOULE, D. C., and RAMSAY, D. A., 1981, *Canad. J. Phys.*, **59,** 1965.
GOLBY, J. A., and BUTCHER, R. J., 1984, *J. molec. Spectrosc.*, **107,** 292.
GOUGH, T. E., ORR, B. J., and SCOLES, G., 1983, *J. molec. Spectrosc.*, **99,** 143.
HALONEN, L., and DUXBURY, G., 1985, *J. chem. Phys.* (in the press).
HALONEN, L., KAUPPINEN, J., and CALDOW, G. L., 1984, *J. chem. Phys.*, **81,** 2257.
HARADA, K., TANAKA, K., and TANAKA, T., 1983, *J. molec. Spectrosc.*, **98,** 349.
HARADA, K., HATANAKA, M., INAYOSHI, A., TANAKA, K., and TANAKA, T., 1984, *J. molec. Spectrosc.*, **108,** 249.
HENNINGSEN, J. O., 1980, *J. molec. Spectrosc.*, **83,** 70.
HENNINGSEN, J. O., 1982, *J. molec. Spectrosc.*, **91,** 430.
HERLEMONT, F., LEMAIRE, J., HOURIEZ, J., and THIBAULT, J., 1973, *C. r. hebd. Séanc. Acad. Sci., Paris*, B, **276,** 733.
HERMAN, M., JOHNS, J. W. C., and MCKELLAR, A. R. W., 1979, *Can. J. Phys.*, **57,** 397.
HERMAN, M., JOHNS, J. W. C., and MCKELLAR, A. R. W., 1982, *J. molec. Spectrosc.*, **95,** 405.
HOUGEN, J. T., 1975, *J. molec. Spectrosc.*, **54,** 447.
HOY, A. R., JOHNS, J. W. C., and MCKELLAR, A. R. W., 1975, *Can. J. Phys.*, **53,** 2039.
IBISCH, E., and ANDRESEN, U., 1980, *Z. Naturf.* (a), **35,** 1020.

IEKI, M., KUMAMOTO, E., KAWAGUCHI, K., YAMADA, C., TANAKA, T., and HIROTA, E., 1978, *J. molec. Spectrosc.*, **71,** 229.
JACOX, M. E., and MILLIGAN, D. E., 1973, *J. molec. Spectrosc.*, **48,** 536.
JACOX, M. E., and MILLIGAN, D. E., 1975 a, *J. molec. Spectrosc.*, **56,** 333.
JACOX, M. E., and MILLIGAN, D. E., 1975 b, *J. molec. Spectrosc.*, **58,** 142.
JOHNS, J. W. C., and OLSON, W. B., 1971, *J. molec. Spectrosc.*, **39,** 47.
JOHNS, J. W. C., and MCKELLAR, A. R. W., 1973, *J. molec. Spectrosc.*, **48,** 354.
JOHNS, J. W. C., and MCKELLAR, A. R. W., 1975, *J. chem. Phys.*, **63,** 1682.
JOHNS, J. W. C., MCKELLAR, A. R. W., OKA, T., and ROMHELD, M., 1975 a, *J. chem. Phys.*, **62,** 1488.
JOHNS, J. W. C., MCKELLAR, A. R. W., and TROMBETTI, A., 1975 b, *J. molec. Spectrosc.*, **55,** 131.
JOHNS, J. W. C., and MCKELLAR, A. R. W., 1977 a, *J. molec. Spectrosc.*, **64,** 327.
JOHNS, J. W. C., and MCKELLAR, A. R. W., 1977 b, *J. chem. Phys.*, **66,** 1217.
JOHNS, J. W. C., MCKELLAR, A. R. W., and RIGGIN, M., 1977, *J. chem. Phys.*, **67,** 2427.
JOHNS, J. W. C., and MCKELLAR, A. R. W., 1978, *Can. J. Phys.*, **56,** 737.
JOHNS, J. W. C., MCKELLAR, A. R. W., and WEINBERGER, E., 1983, *Can. J.Phys.*, **61,** 1106.
JOHNSON, D. R., and POWELL, F. X., 1970, *Science*, **169,** 679.
JOHNSTON, L. H., SRIVASTAVA, R. P., and LEES, R. M., 1980, *J. molec. Spectrosc.*, **84,** 1.
JOHNSTON, L. H., RAJU, S. R., SUDHAKARAN, G. R., and LEES, R. M., 1982, *J. molec. Spectrosc.*, **91,** 503.
KAWAGUCHI, K., YAMADA, C., TANAKA, T., and HIROTA, E., 1977, *J. molec. Spectrosc.*, **64,** 125.
KAWAGUCHI, K., and TANAKA, T., 1977, *J. molec. Spectrosc.*, **68,** 125.
KIVELSON, D., 1957, *J. chem. Phys.*, **26,** 215.
KREINER, W. A., ORR, B. J., ANDRESEN, U., and OKA, T., 1977, *Phys. Rev.* A., **55,** 2297.
KREINER, W. A., OKA, T., and ROBIETTE, A. G., 1978, *J. chem. Phys.*, **68,** 3236.
KROTO, H. W., 1982, *Chem. Soc. Rev.*, **11,** 435.
KUZE, H., AMANO, T., and SHIMIZU, T., 1982, *J. chem. Phys.*, **77,** 714.
LANDSBERG, B. M., MERER, A. J., and OKA, T., 1977, *J. molec. Spectrosc.*, **67,** 459.
LAHAYE, J. G., LAMBEAU, C. H., FAYT, A., LEMAIRE, J., HERLEMONT, F., and LYSZYK, M., 1985, *Applied Optics*, **24,** 1657.
LAUGHTON, D., FREUND, S. M., and OKA, T., 1976, *J. molec. Spectrosc.*, **62,** 263.
LUNTZ, A. C., BREWER, R. G., FOSTER, K. L., and SWALEN, J. D., 1969, *Phys. Rev. Lett.*, **23,** 951.
LUNTZ, A. C., 1971, *Chem. Phys. Lett.*, **11,** 186.
LUNTZ, A. C., SWALEN, J. D., and BREWER, R. G., 1972, *Chem. Phys. Lett.*, **14,** 512.
MACKE, B., and LEGRAND, J., 1974, *J. Phys.* B, *Atom. molec. Phys.*, **7,** 865.
MAKI, A. G., and FREUND, S. M., 1976, *J. molec. Spectrosc.*, **62,** 90.
MAKI, A. G., and FREUND, S. M., 1977, *J. molec. Spectrosc.*, **66,** 493.
MAKI, A. G., and FREUND, S. M., 1982, *J. molec. Spectrosc.*, **93,** 433.
MARSHALL, M. D., and MUENTER, J. S., 1980, *J. molec. Spectrosc.*, **83,** 279.
MARSHALL, M. D., and MUENTER, J. S., 1981, *J. molec. Spectrosc.*, **85,** 322.
MATSUSHIMA, F., MORITA, M., HONGAL, Y., and SHIMIZU, T., 1981, *Appl. Phys.*, **24,** 219.
MATSUMURA, K., TANAKA, K., YAMADA, C., and TANAKA, T., 1980, *J. molec. Spectrosc.*, **80,** 209.
MCCOMBIE, J., and DUXBURY, G., 1985, (to be published).
MEYER, F., DUPRE, J., MEYER, C., DE VLEESCHOUWER, M., LAHAYE, J.-G., and FAYT, A., 1982, *Int. J. I. R. Millimetre Waves*, **3,** 83.
MILLS, I. M., WATSON, J. K. G., and SMITH, W. K., 1969, *Molec. Phys.*, **16,** 329.
MILLS, I. M., MCKELLAR, A. R. W., and DUXBURY, G., 1981, *Faraday Discuss. Chem. Soc.* No. 71, pp. 321–323.
MINGUZZI, P., TONELLI, M., CAROZZI, A., and DI LIETO, A., 1982, *J. molec. Spectrosc.*, **96,** 294.
MITO, A., SAKAI, J., and KATAYAMA, M., 1984 a, *J. molec. Spectrosc.*, **103,** 26.
MITO, A., SAKAI, J., and KATAYAMA, M., 1984 b, *J. molec. Spectrosc.*, **105,** 410.
MIZUSHIMA, M., and VENKATESWARLU, P., 1953, *J. chem. Phys.*, **21,** 705.
MUENTER, A. A., and DYKE, T. R., 1975, *J. chem. Phys.*, **63,** 1224.
NAKAGAWA, K., NAKAGAWA, T., UEDA, Y., and KUCHITZA, K., 1976, *J. molec. Spectrosc.*, **63,** 547.
OKA, T., 1973, *Adv. Atom molec. Phys.*, **9,** 127.
OKA, T., 1976, *Molecular Spectroscopy: Modem Research*, Vol. 2, edited by K. N. Rao (New York: Academic Press), p. 229.
ORR, B. J., and OKA, T., 1977 a, *Appl. Phys. Lett.*, **30,** 468.
ORR, B. J., and OKA, T., 1977 b, *J. molec. Spectrosc.*, **66,** 302.
ORR, B. J., and OKA, T., 1980, *Appl. Phys.*, **21,** 293.

OZIER, I., 1971, *Phys. Rev. Lett.*, **27,** 1329.
PETERSEN, F. R., WELLS, J. S., SIEMSEN, K. J., ROBINSON, A. M., and MUKI, A. G., 1984, *J. molec. Spectrosc.*, **105,** 324.
RACKLEY, S. A., and BUTCHER, R. J., 1980, *Molec. Phys.*, **39,** 1265.
RACKLEY, S. A., BUTCHER, R. J., ROMHELD, M., FREUND, S. M., and OKA, T., 1982, *J. molec. Spectrosc.*, **92,** 203.
REINARTZ, J. M. L. J., and DYMANUS, A., 1974, *Chem. Phys. Lett.*, **16,** 576.
ROBIETTE, A. G., and DUNCAN, J. L., 1983, *Ann. Rev. phys. Chem.*, **34,** 245.
SAKAI, J., and KATAYAMA, M., 1975, *Chem. Phys. Lett.*, **35,** 395.
SAKAI, J., and KATAYAMA, M., 1976, *Appl. Phys. Lett.*, **28,** 119.
SAKURAI, K., UEHARA, K., TAKAMI, M., and SHIMODA, K., 1967, *J. phys. Soc. Japan*, **23,** 103.
SANDHOLM, S. T., and SCHWENDEMAN, R. H., 1983, *J. chem. Phys.*, **78,** 3476.
SASADA, H., HASEGAWA, Y., AMANO, T., and SHIMIZU, T., 1982, *J. molec. Spectrosc.*, **96,** 106.
SHIMIZU, F., 1969, *J. chem. Phys.*, **51,** 2754.
SHIMIZU, F., 1970 a, *J. chem. Phys.*, **52,** 3572.
SHIMIZU, F., 1970 b, *J. chem. Phys.*, **53,** 1149.
SHIMIZU, F., 1972, *Chem Phys. Lett.*, **17,** 620.
SHIMIZU, F., 1975 a, *J. phys. Soc. Japan*, **38,** 293.
SHIMIZU, F., 1975 b, *J. phys. Soc. Japan*, **38,** 1106.
SHIMIZU, F., SHWE, H., and TAMAYAMA, T., 1975, *J. appl. Phys.*, **46,** 258.
SHIMIZU, F., 1975 c, *Japan J, appl. Phys.*, **14,** 521.
SHIMIZU, T., SHIMODA, K., and MINOH, A., 1968, *J. phys. Soc. Japan*, **24,** 1185.
SHIMODA, K., 1973, *Appl. Phys.*, **1,** 77.
SHIMODA,K., UEDA, Y., and IWAHORI, J., 1980 a, *Appl. Phys.*, **21,** 181.
SHIMODA, K., UEDA, Y., and IWAHORI, J., 1980 b, *Appl. Phys.*, **22,** 439.
SHOEMAKER, R. L., STENHOLM, S., and BREWER, R. G., 1974, *Phys. Rev.* A, **10,** 2037.
SINCLAIR, M. W., FOURIKIS, N., RIBES, J. C., ROBINSON, B. J., BROWN, R. D., and GODFREY, P. D., 1973, *Aust. J. Phys.*, **26,** 85.
STARK, J., 1913, *Sber. preuss. Akad. Wiss.*, **47,** 932.
TAKAGI, K., 1984, *Chem. Phys. Lett.*, **112,** 302.
TAKAMI, M., JONES, H., and OKA, T., 1979, *J. chem. Phys.*, **70,** 3557.
TANAKA, K., and TAKANA, T., 1978, *J. molec. Spectrosc.*, **69,** 335.
TANAKA, K., INAYOSHI, A., KIJIMA, K., and TANAKA, T., 1982, *J. molec. Spectrosc.*, **95,** 182.
TANAKA, K., and TANAKA, T., 1983, *J. molec., Spectrosc.*, **98,** 425.
TANAKA, K., ITO, H., HARADA, K., and TANAKA, T., 1984, *J. chem. Phys.*, **80,** 5893.
TANAKA, T., YAMADA, C., and HIROTA, E., 1976, *J. molec. Spectrosc.*, **63,** 142.
TANAKA, T., INAYOSHI, A., KIJIMA, K., HARADA, K., and TANAKA, K., 1982, *Rev. scient. Instrum.*, **53,** 1552.
TOBIN, M. S., SATTLER, J. P., and WOOD, G. L., 1979, *Opt. Lett.*, **4,** 384.
TOYAMA, M., OKA, T., and MORINA, Y., 1964, *J. molec. Spectrosc.*, **13,** 193.
UEDA, Y., and SHIMODA, K., 1975, *Laser Spectroscopy,* edited by S. Haroche, J. C. Pebay-Peyroula, T. W. Hansch and S. E. Harris (Berlin: Springer-Verlag), p. 186.
UEHARA, K., SHIMIZU, T., and SHIMODA, K., 1968, *IEEE Jl quant. Electron.*, **QE-4,** 728.
UEHARA, K., SAKURAI, K., and SHIMODA, K., 1969, *J. phys. Soc. Japan*, **26,** 1018.
VACCARO, P. H., KINSEY, J. L., FIELD, R. W., and DAI, H. L., 1983, *J. chem. Phys.*, **78,** 3659.
WATSON, J. K. G., 1971, *J. molec. Spectrosc.*, **40,** 536.
WATSON, J. K. G., TAKAMI, M., and OKA, T., 1979, *J. chem. Phys.*, **70,** 5376.
WEBER, W. H., and TERHUNE, R. W., 1981, *Opt. Lett.*, **6,** 455.
WEBER, W. H., and TERHUNE, R. W., 1983 a, *J. chem. Phys.*, **78,** 6422.
WEBER, W. H., and TERHUNE, R. W., 1983 b, *J. chem. Phys.*, **78,** 6437.
WHITFORD, B. G., SIEMSEN, K. J., RICCIUS, H. D., and HAINES, G. R., 1975, *Opt. Commun.*, **14,** 70.
WOFSY, S. C., MUENTER, J. S., and KLEMPERER, W., 1971, *J. chem. Phys.*, **55,** 2014.
WONG. M., JOHNS, J. W. C., and MCKELLAR, A. R. W., 1982, *J. molec. Spectrosc.*, **94,** 79.
YAMADA, C., and HIROTA, E., 1977, *J. molec. Spectrosc.*, **64,** 31.